Rapid plate motion changes: observations and geodynamic interpretations

Hans-Peter Bunge

Ludwig-Maximilians University (LMU) München

L. Colli, I. Stotz, M. C. Bianchi, M. Smethurst, S. Clark, G. Iaffaldano, A. Tassara, F. Guillocheau

Collège de France
November 21st, 2014

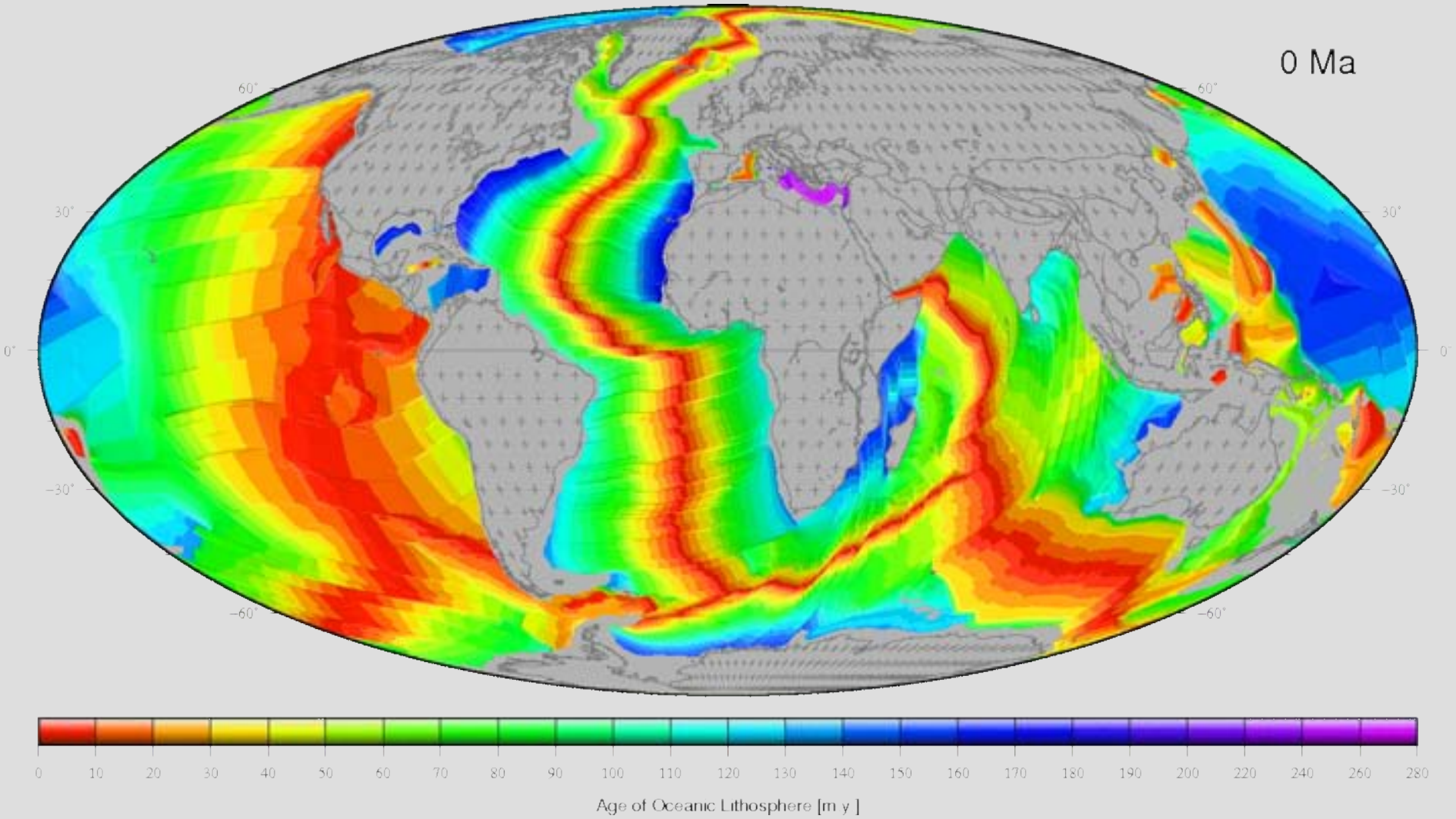

redrawn from Mueller et al., (2008)

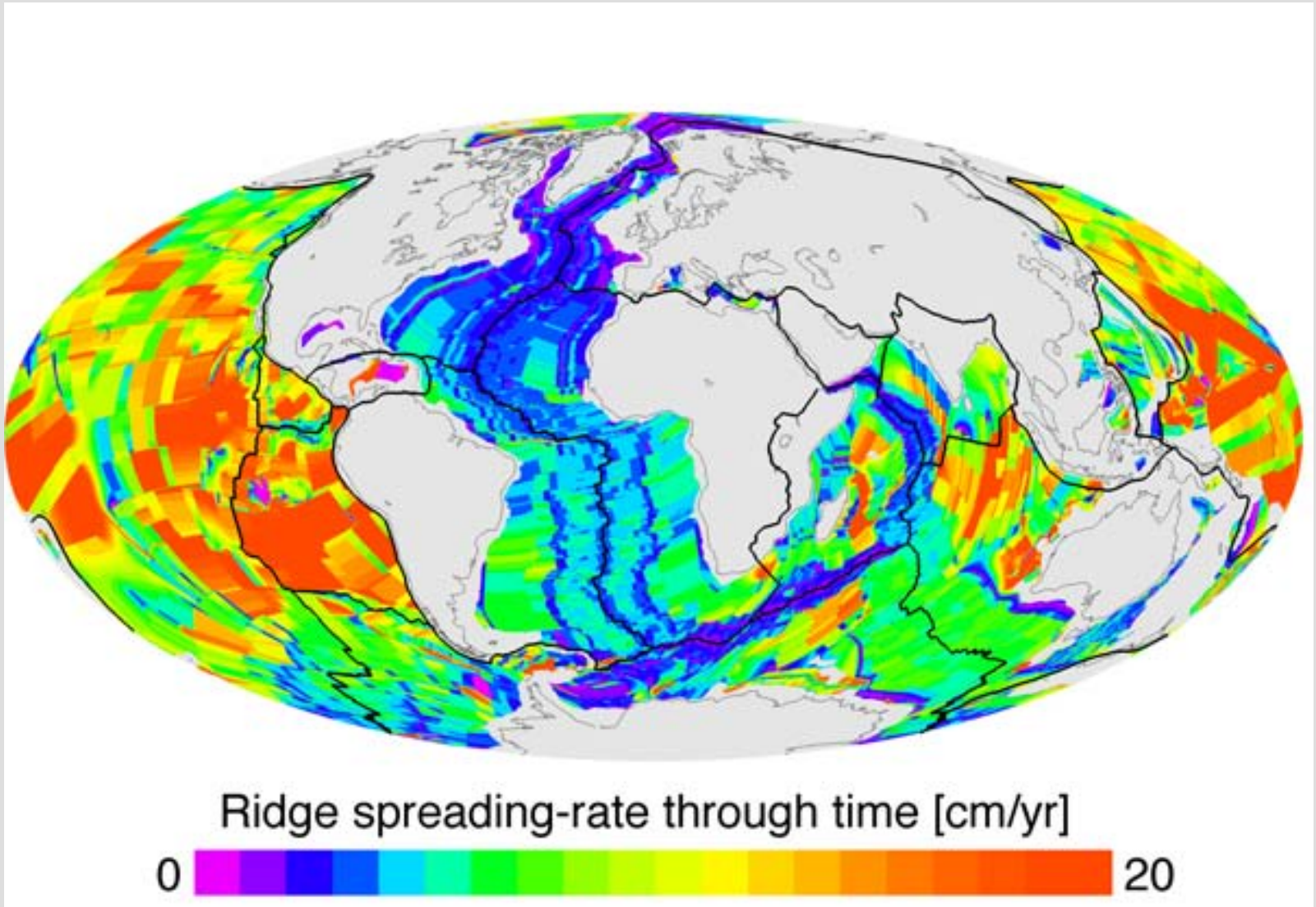

Iaffaldano & Bunge (2015) redrawn from Mueller et al., (2008)

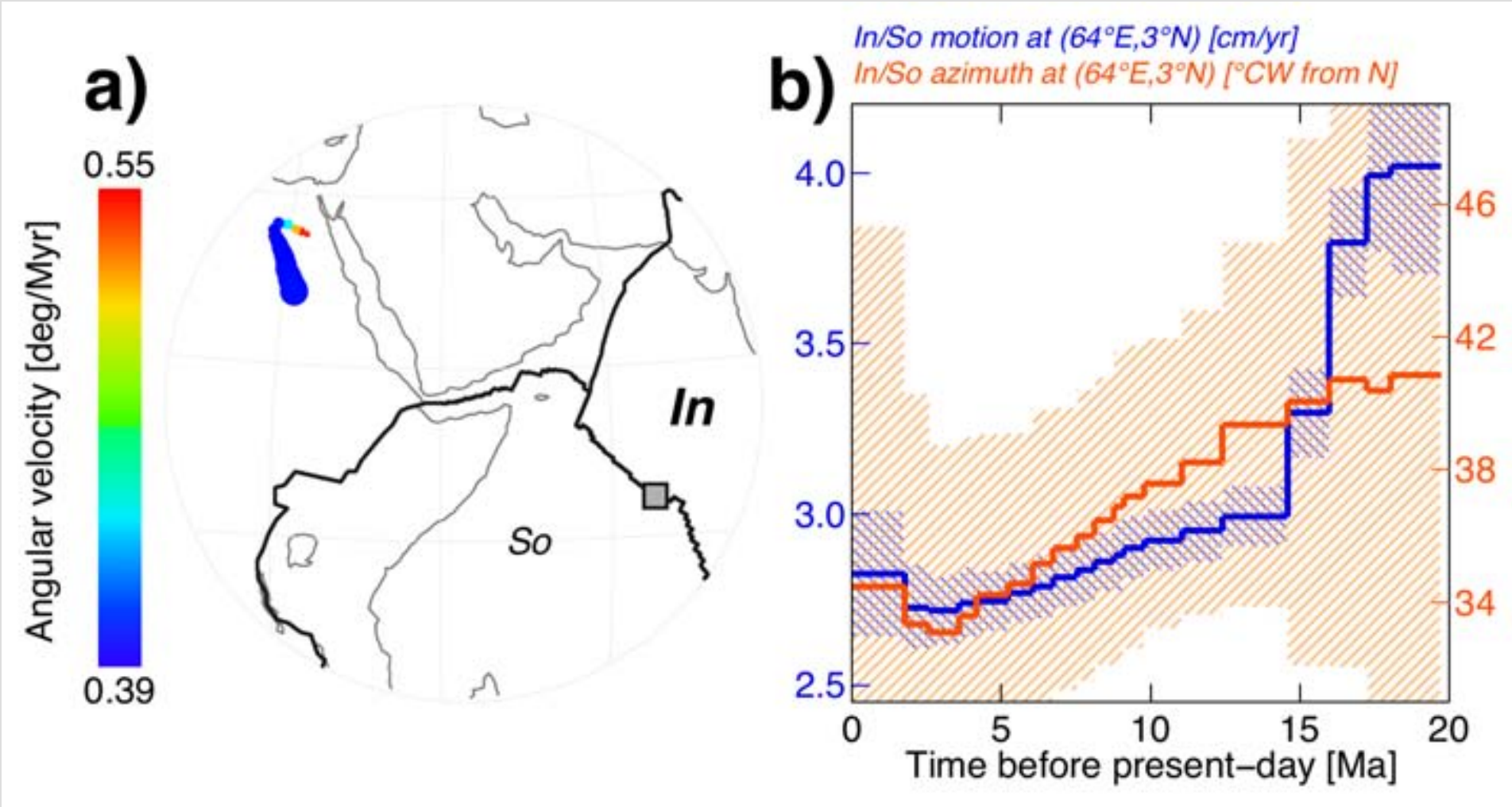

Iaffaldano & Bunge (2015)

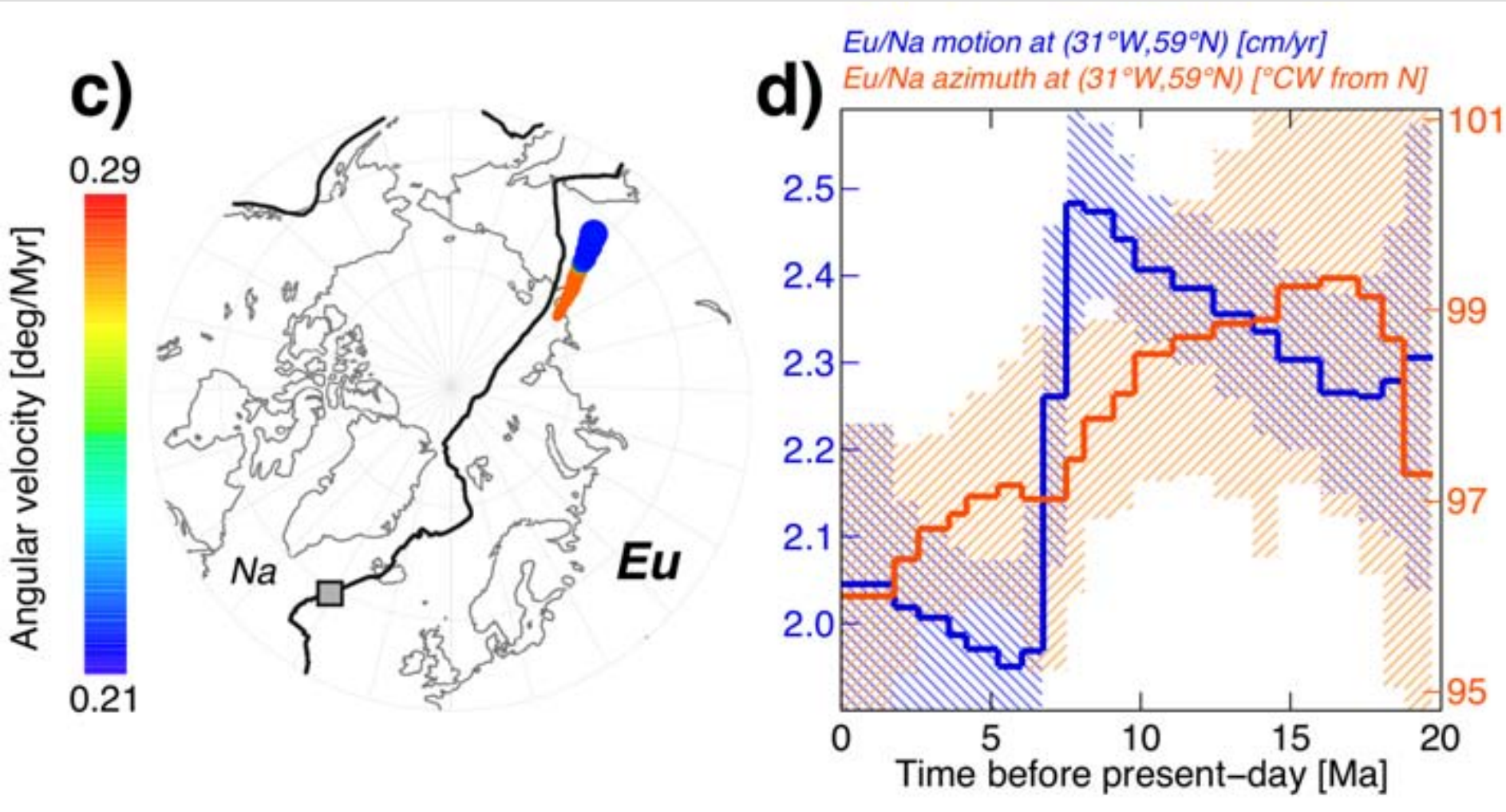

Iaffaldano & Bunge (2015)

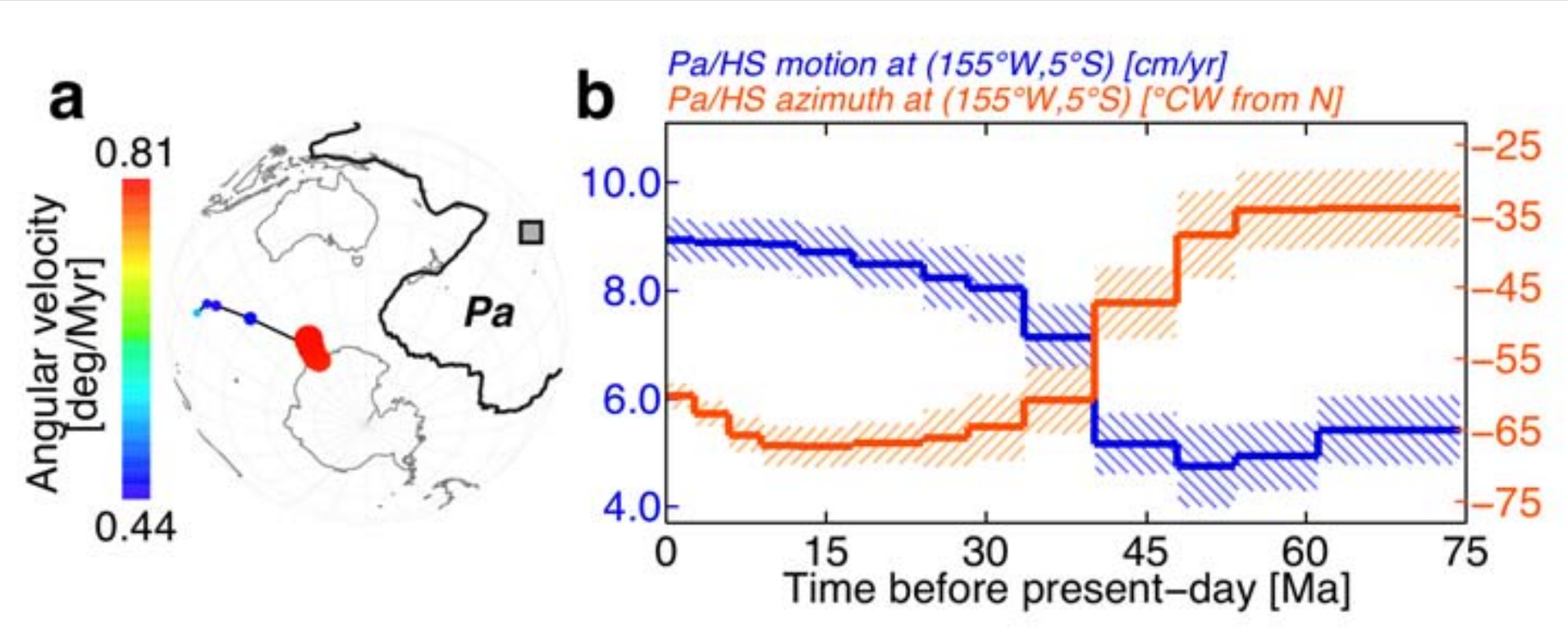

Iaffaldano & Bunge (2015)

finite rotations of **Wessel & Kroenke (2008)**

Hotspot Motion (a likely case for Hawaii)

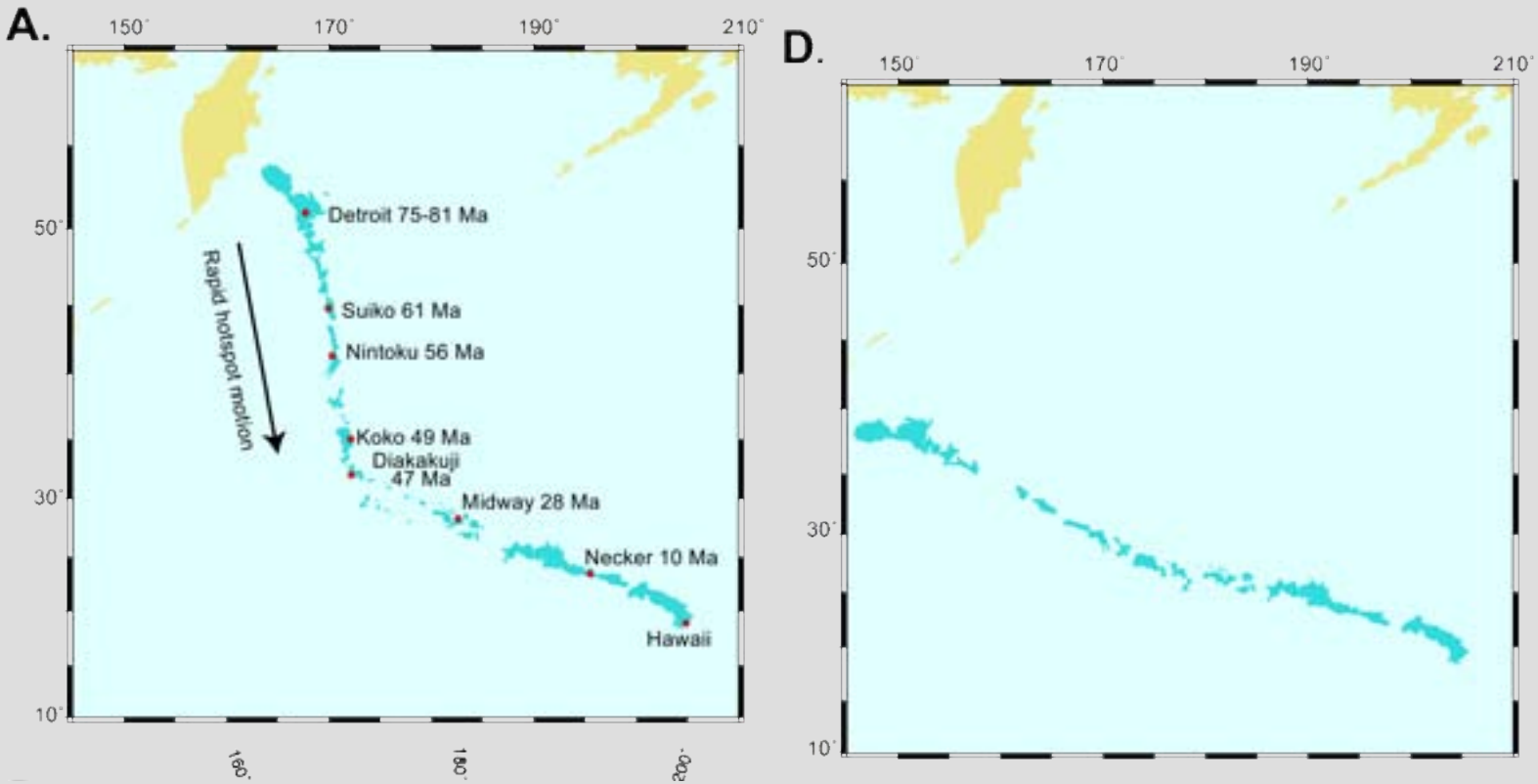

Hawaii Hotspot track (observed, left) and corrected (right) for paleomagnetically inferred plume drift

Tarduno et al. (2009)

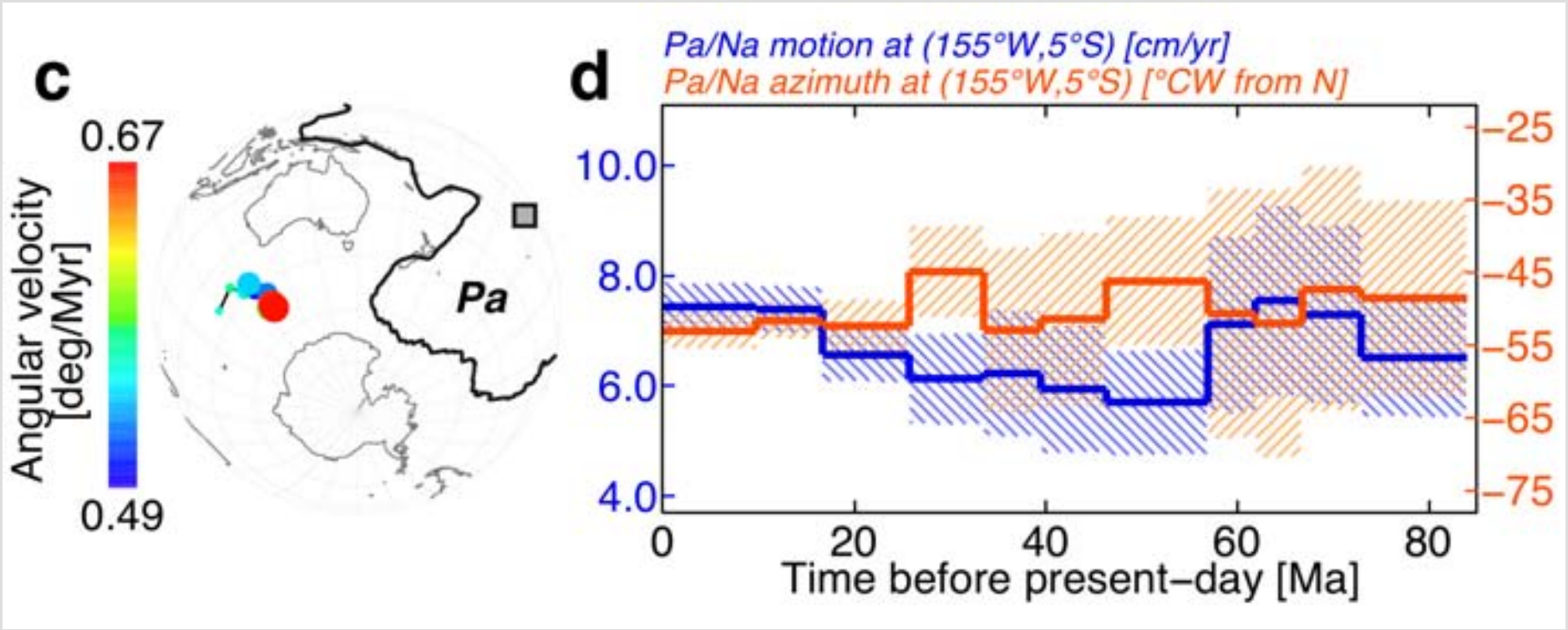

Iaffaldano & Bunge (2015)

finite rotations of **Doubrovine & Tarduno (2008)**

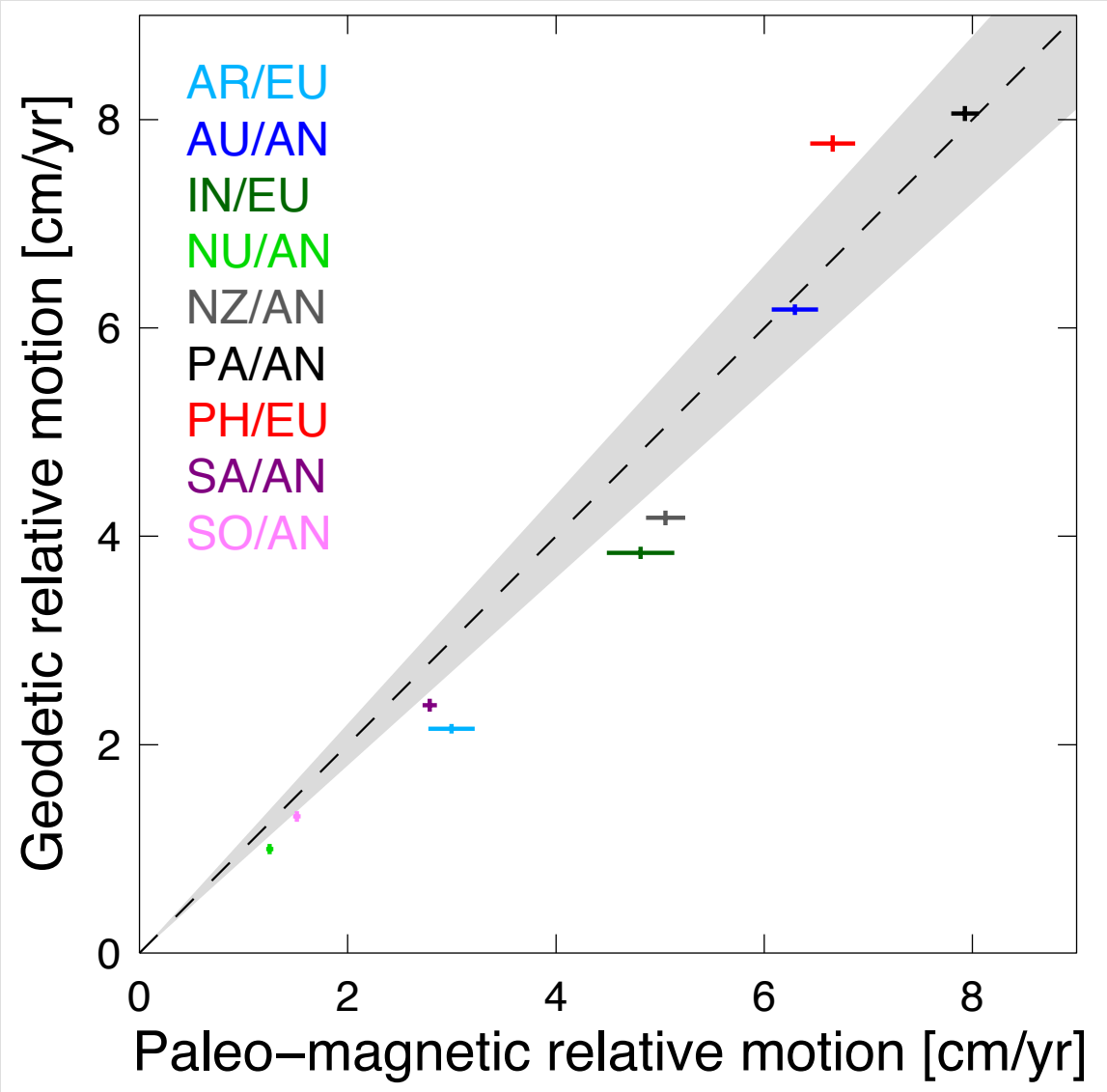

Iaffaldano & Bunge (2015)

Time Scales (thermal)

advective and diffusive time scale

$$\tau_a = \frac{D}{u}, \qquad \tau_c = \frac{D^2}{\kappa}$$

advection dominates conduction

$$Pe = \frac{\tau_c}{\tau_a} = \frac{Du}{\kappa} >> 1$$

with

τ_a	advection time scale
τ_c	diffusion time scale
D	mantle depth
u	typical plate velocity
κ	thermal diffusivity
Pe	Peclet number

Advection dominates in the mantle away from thermal boundary layers, making τ_a the relevant time scale.
Buoyancies evolve on time scales of order 100 Myrs.

Time scale of evolving buoyancies from convection models

- initialize convection model
- run with one plate stage for a long time
- change to a new plate stage
- run with new plate stage for a long time
- monitor the evolving cross correlation

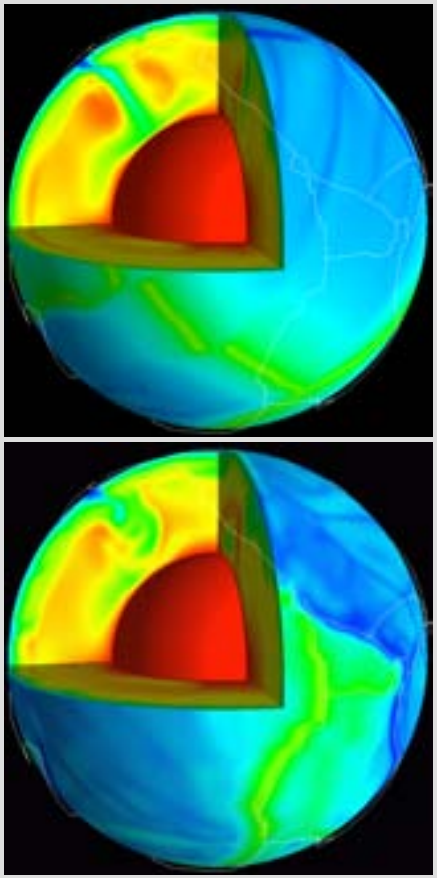

Time scale of evolving buoyancies from convection models

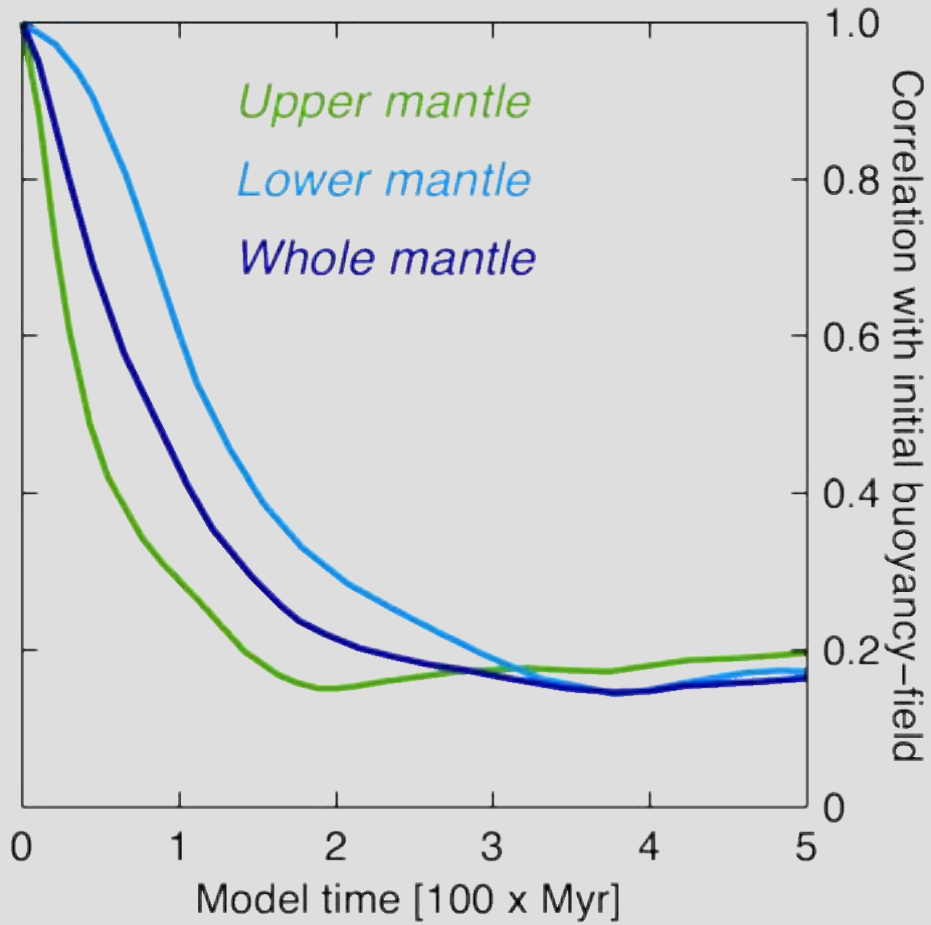

Time scale of evolving buoyancies from convection models

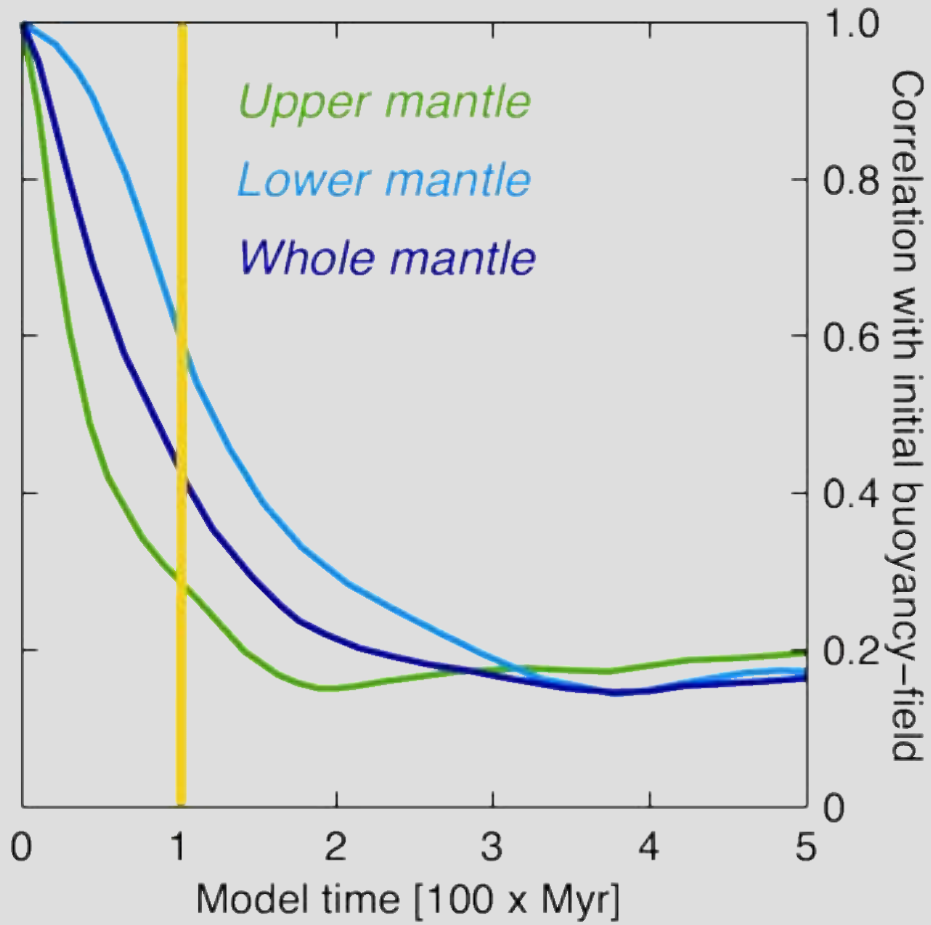

Time Scales (momentum)

momentum diffusion

$$\tau_m = D^2 \varrho / \mu$$

with

τ_m	diffusion time scale
ϱ	mantle density
D	mantle depth
μ	mantle viscosity

mantle flow comes to a halt in under a second if all buoyancy forces were suddenly removed

see, for instance, **Forte (2007)**

Time Scale Momentum Diffusion

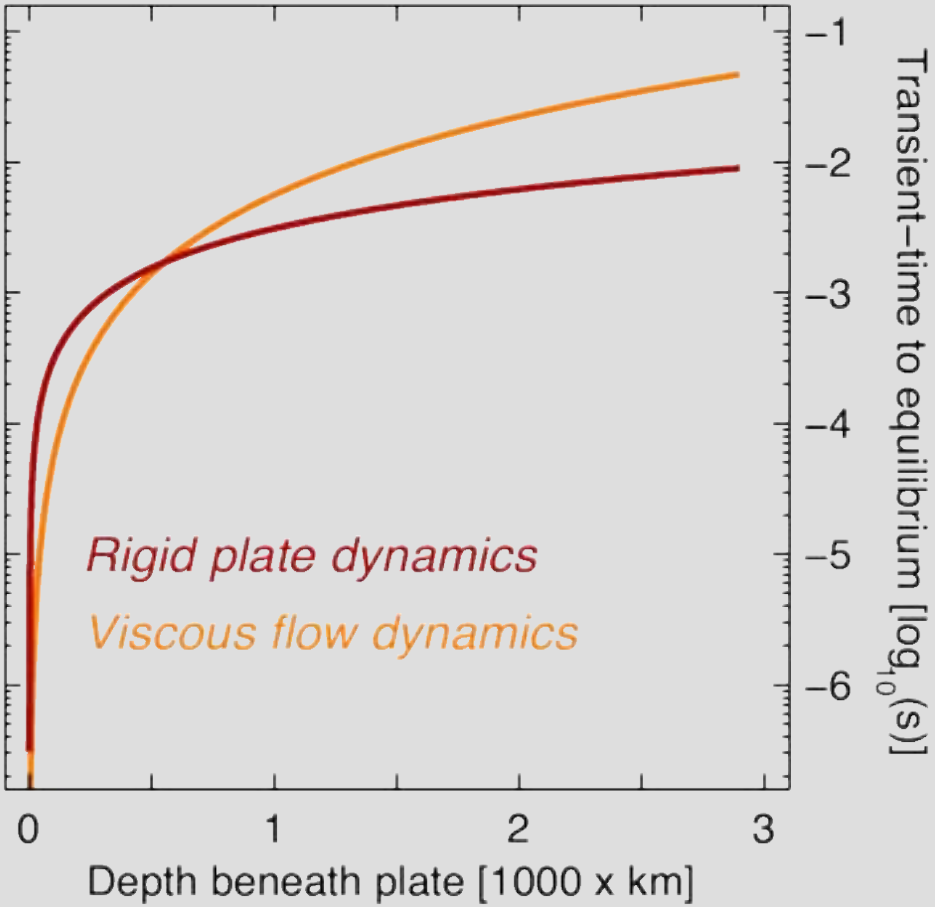

Iaffaldano & Bunge (2015)

Time Scale Momentum Diffusion

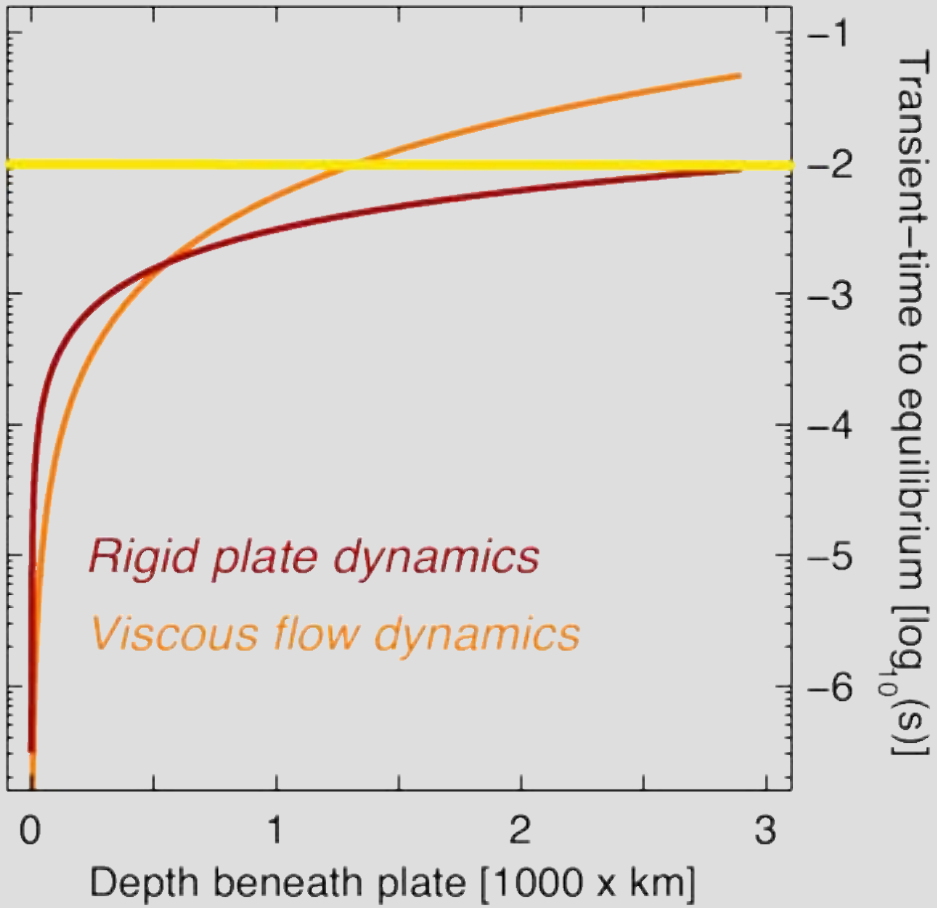

Iaffaldano & Bunge (2015)

Tectonic force balance

$$\sum F_i = ma$$

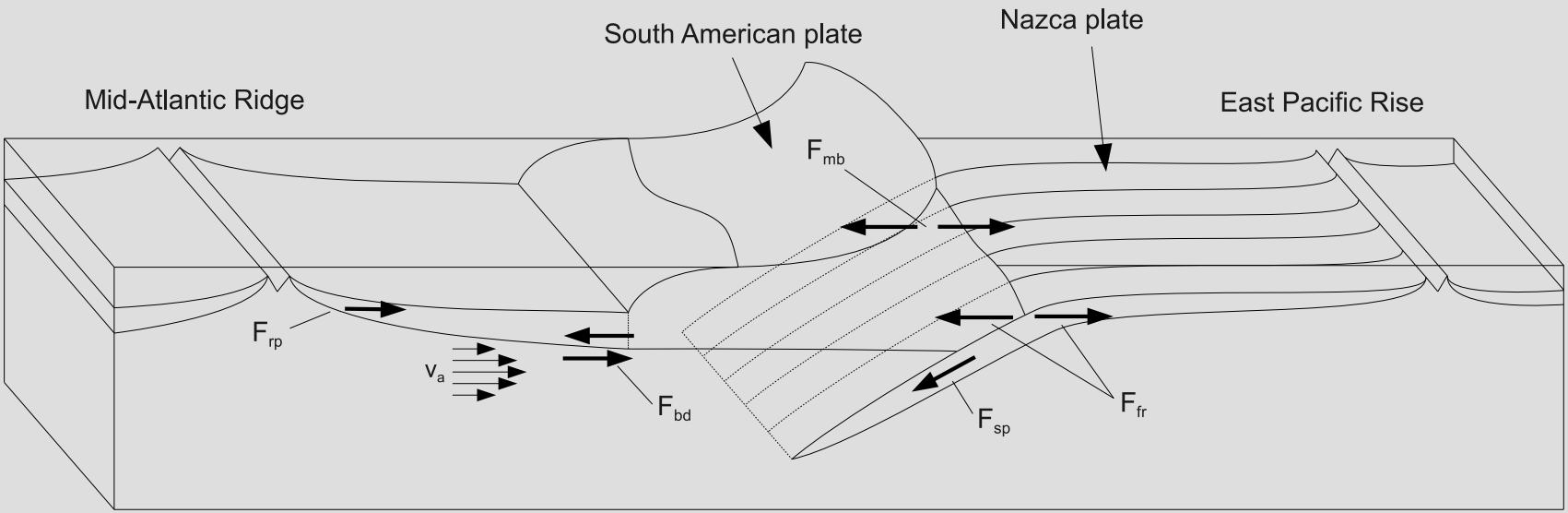

redrawn from Forsyth & Uyeda (1975)

Tectonic force balance

$$\sum F_i = m\cancel{a}$$

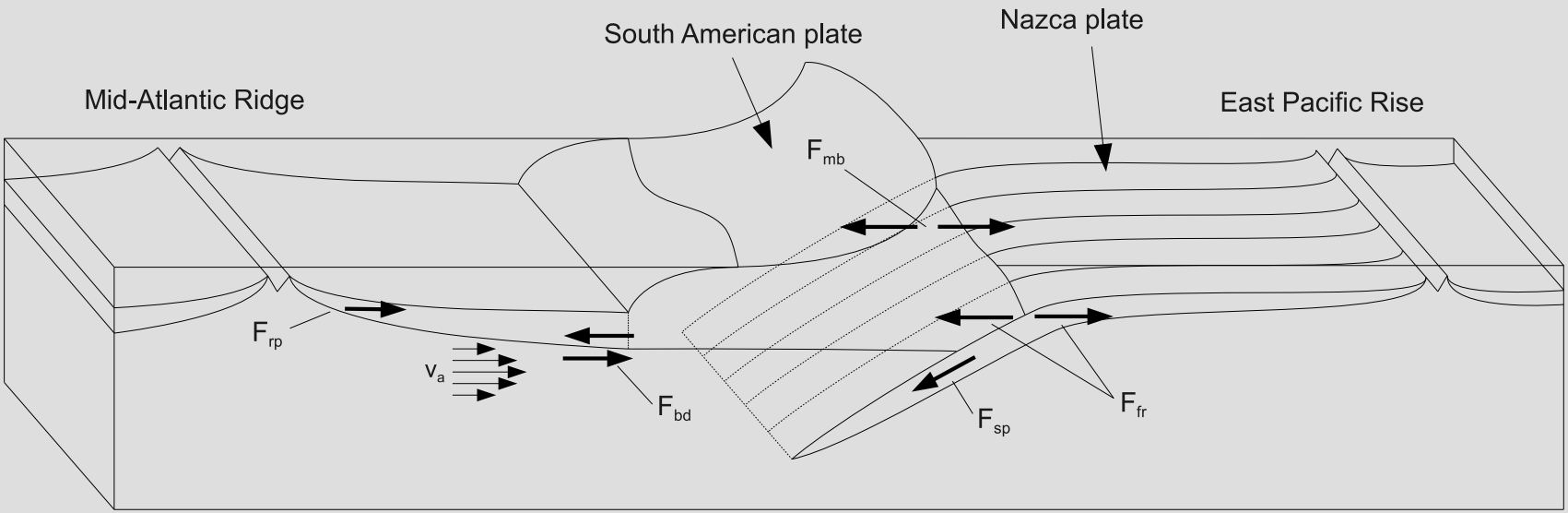

redrawn from Forsyth & Uyeda (1975)

Tectonic force balance

$$\sum F_i = 0$$

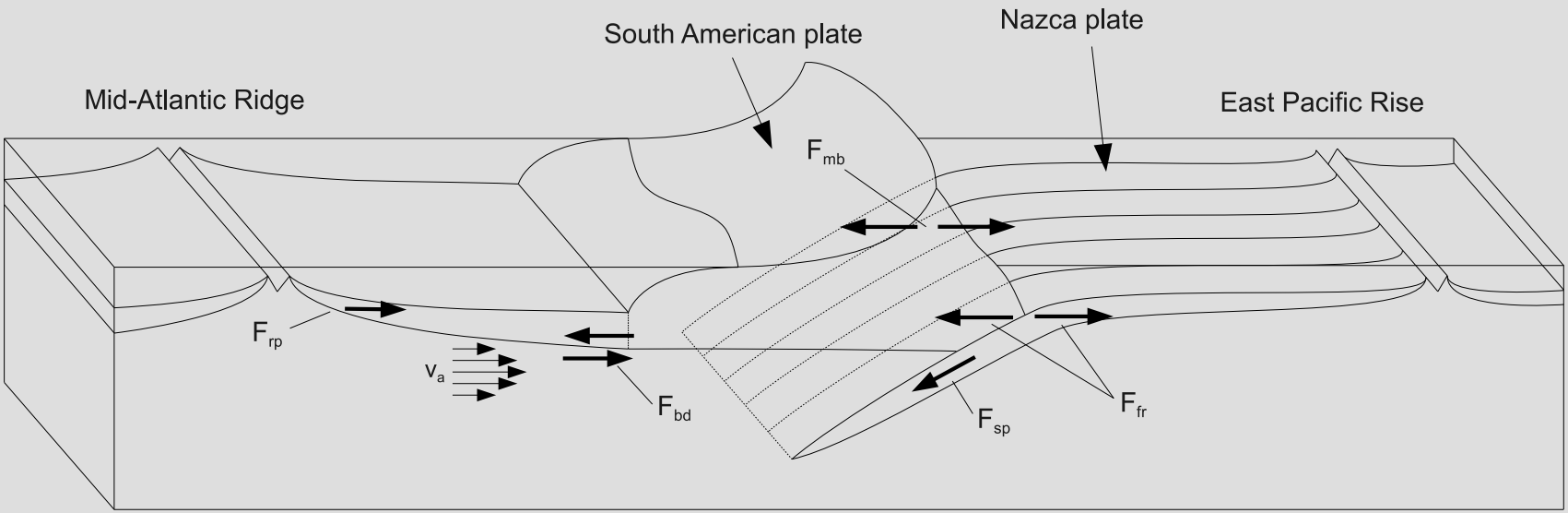

redrawn from Forsyth & Uyeda (1975)

Tectonic force balance

$$\sum F_i = 0$$

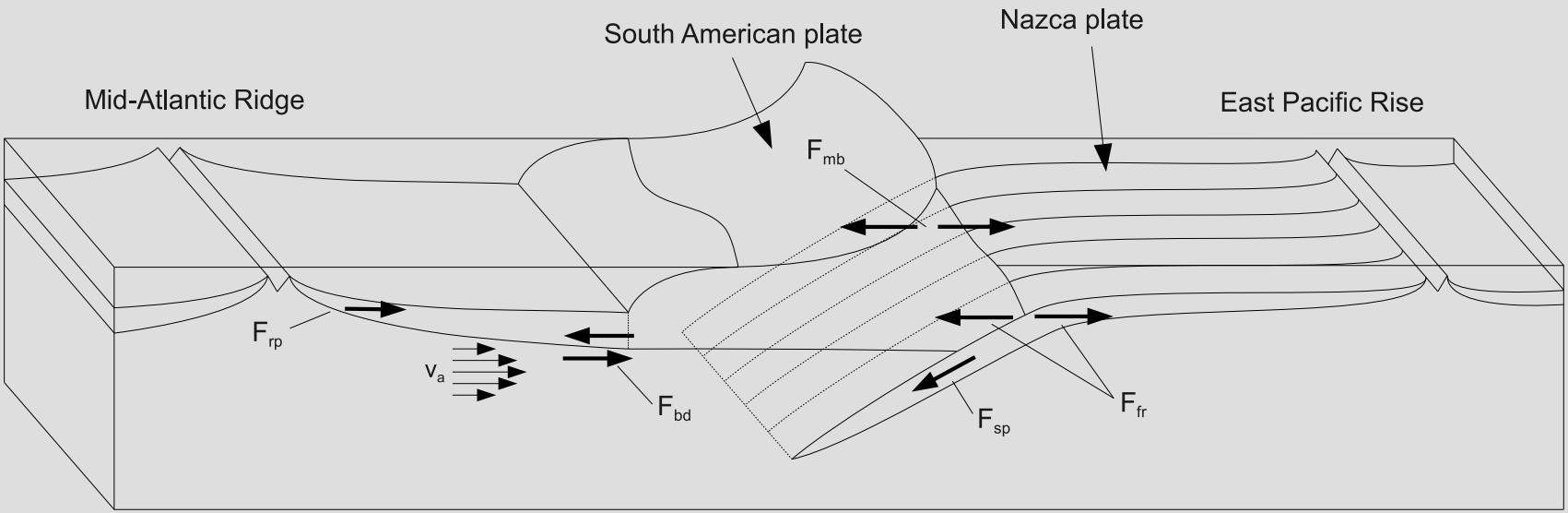

redrawn from Forsyth & Uyeda (1975)

Tectonic force balance

$$F_{rp} + F_{fr} + F_{mb} + F_{bd} = 0$$

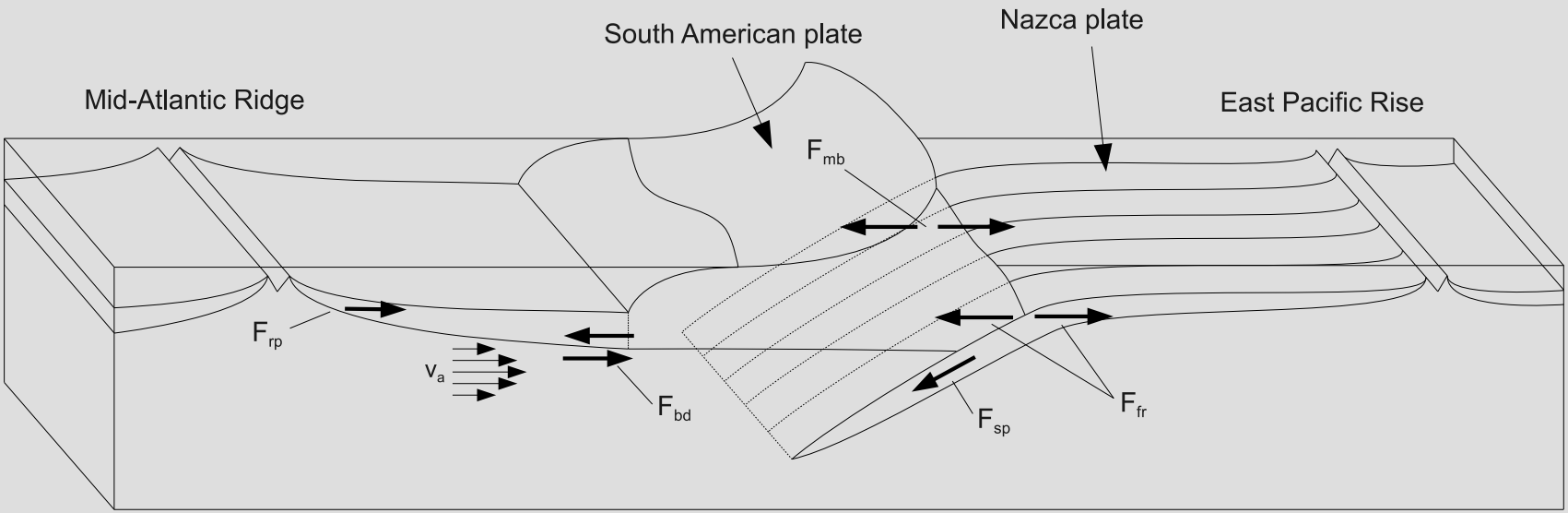

redrawn from Forsyth & Uyeda (1975)

Plate Motion Changes

While plate motions sample the *sum of all torques* at a certain point in time, plate–motion changes sample *torque variations* that have already been *re–equilibrated.*

It is often easier to assess *variations* of torques rather than the *sum* of all torques.

Plate Motion Changes

While plate motions sample the *sum of all torques* at a certain point in time, plate–motion changes sample *torque variations* that have already been *re–equilibrated.*

It is often easier to assess *variations* of torques rather than the *sum* of all torques.

- **Neogene**
  South Atlantic Spreading Variations

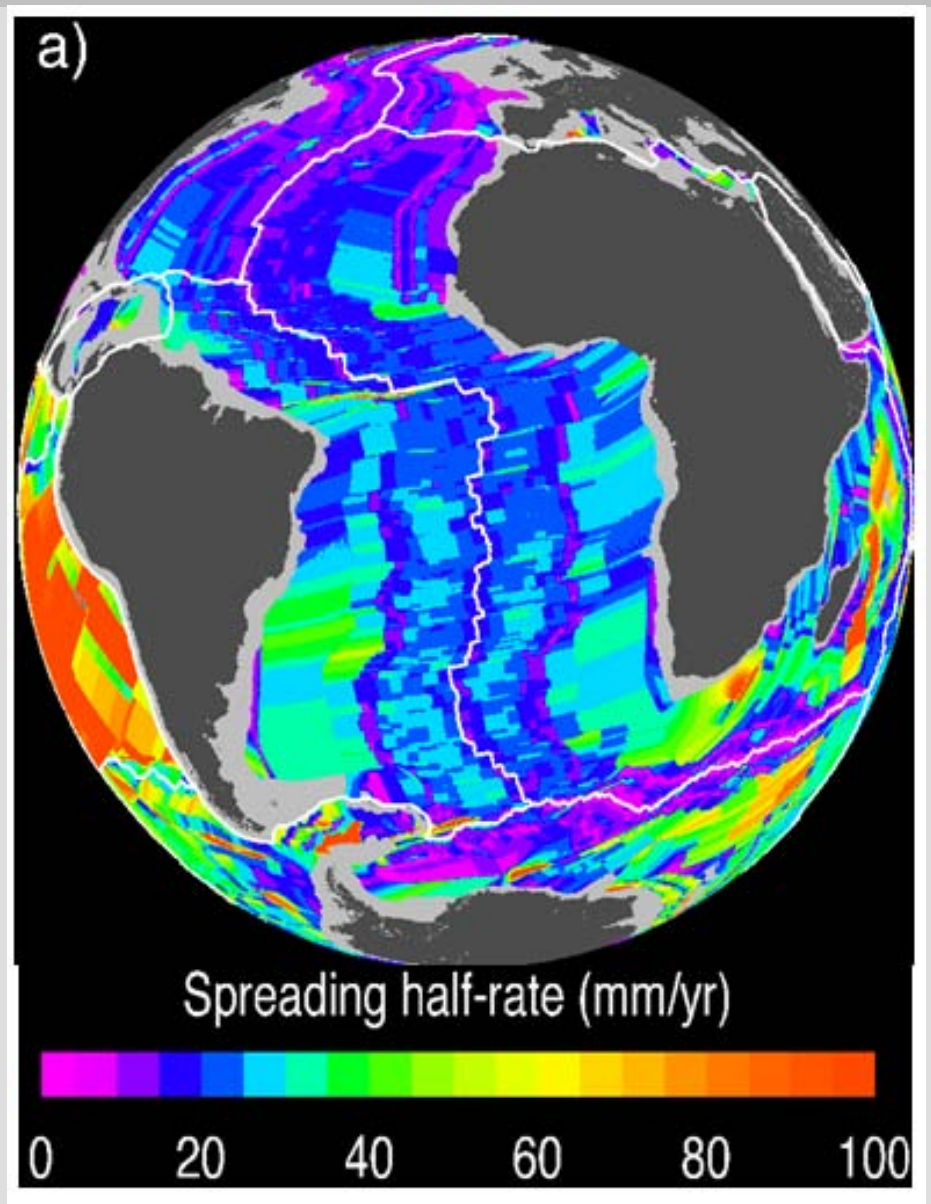

- **Neogene**
  South Atlantic Spreading Variations

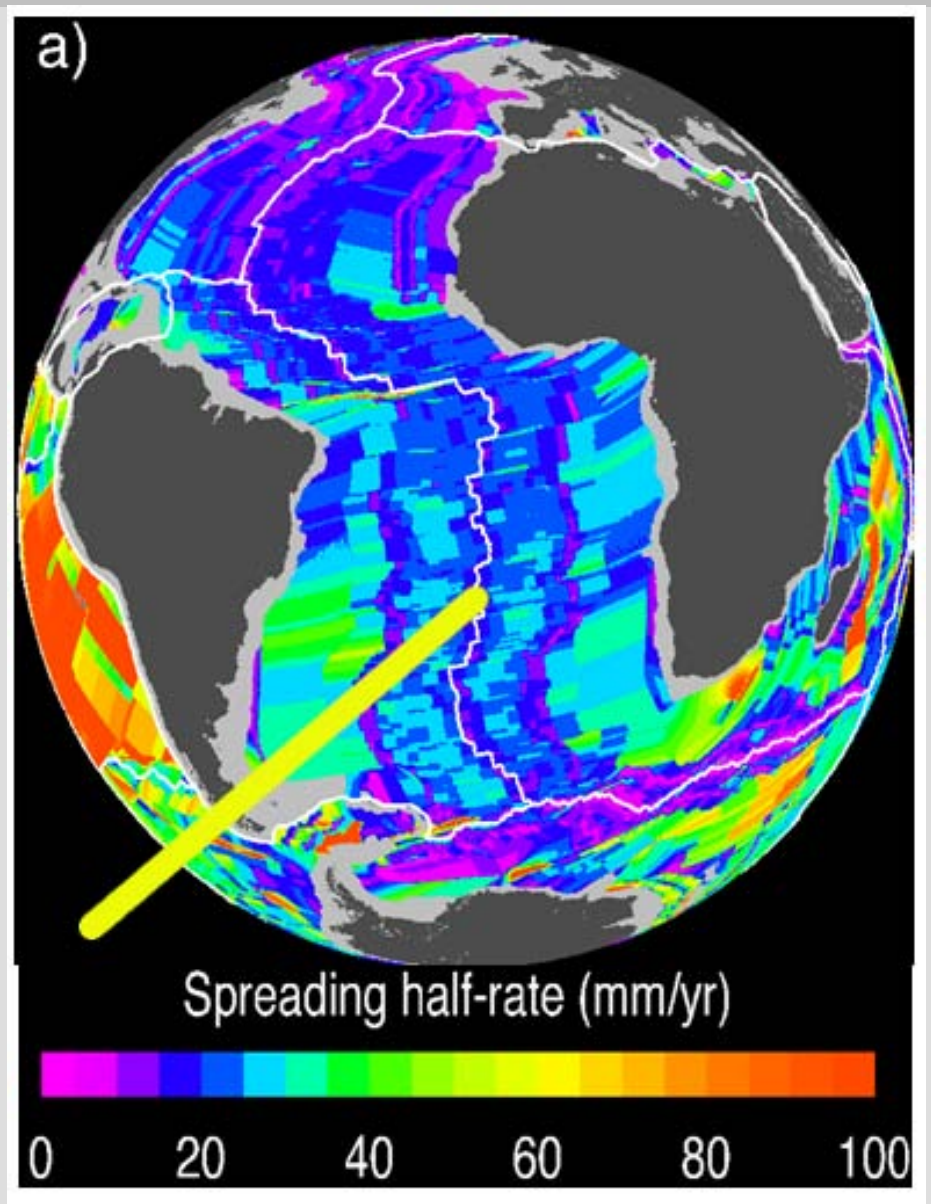

Figure from **Sempere et al. (2008)**, see also *Oncken et al.* (2006) and many others

Geologic estimates of Paleo-Andean elevation

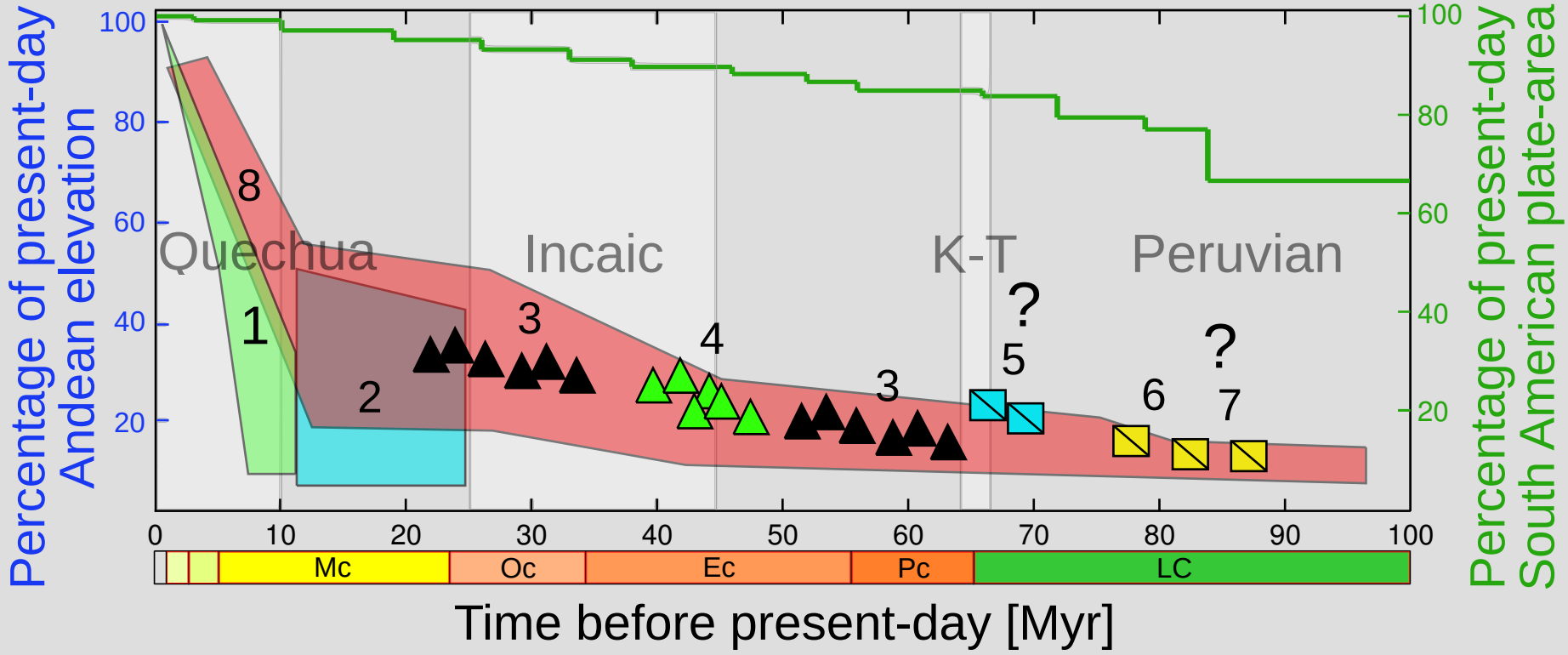

Colli et al. (2014)

Global **Neotectonic Models** coupled to **Mantle Circulation Models** that include buoyancies from a subduction history

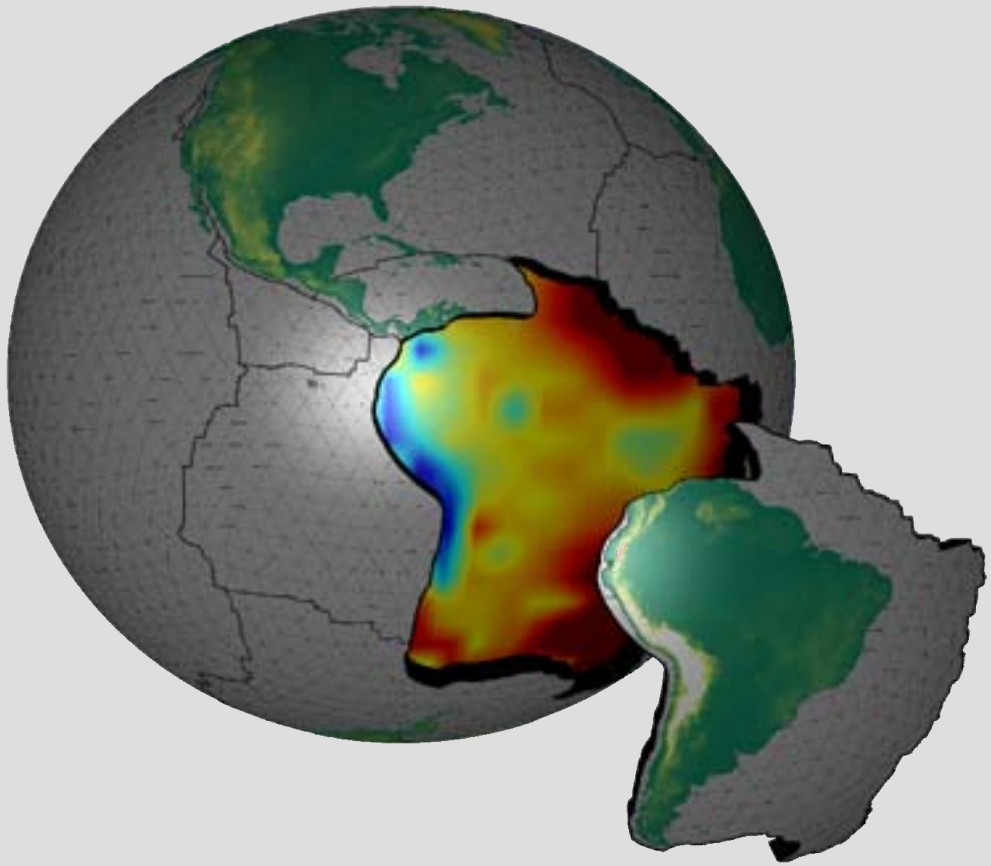

e.g., **Iaffaldano et al. (2006), Iaffaldano & Bunge (2006,2009), Iaffaldano et al. (2011), Austermann & Iaffaldano (2013**

Global **Neotectonic Models** coupled to **Mantle Circulation Models** that include buoyancies from a subduction history

Topography

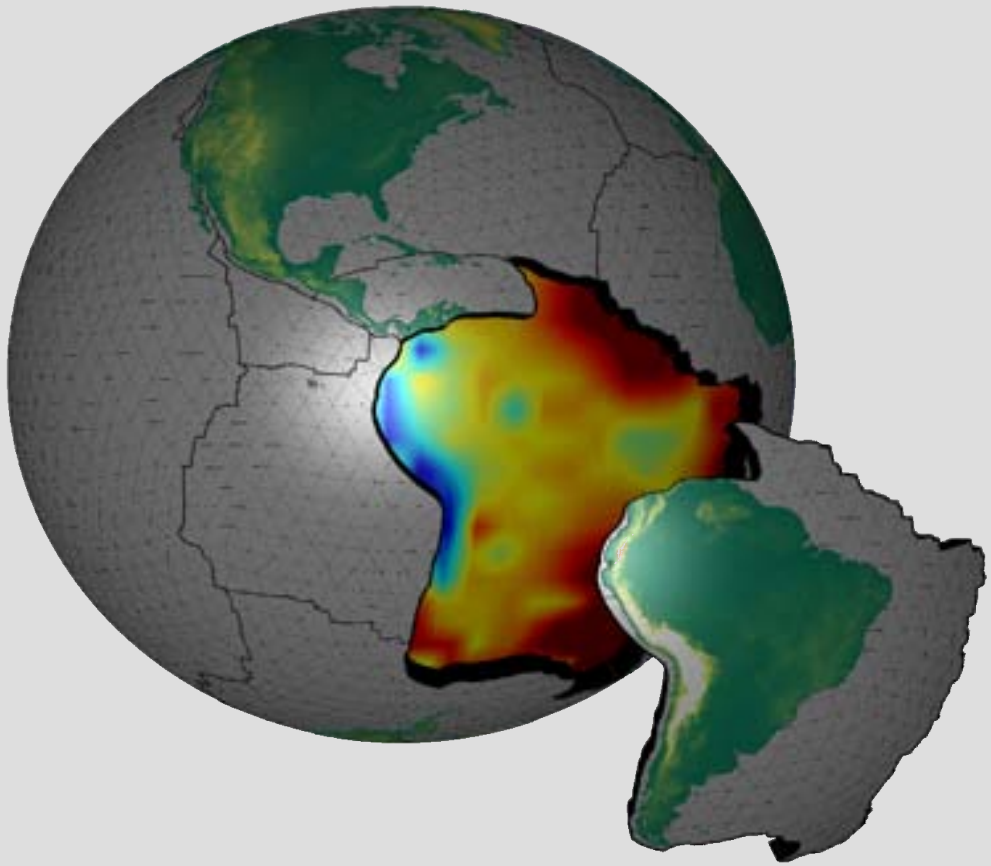

e.g., **Iaffaldano et al. (2006), Iaffaldano & Bunge (2006,2009), Iaffaldano et al. (2011), Austermann & Iaffaldano (2013**

Global **Neotectonic Models** coupled to **Mantle Circulation Models** that include buoyancies from a subduction history

Realistic Strength Envelope

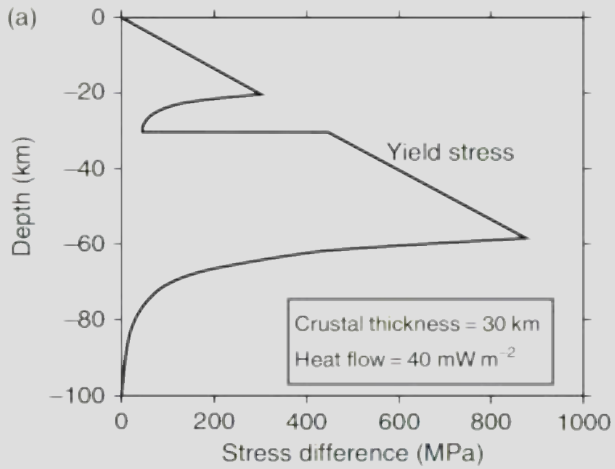

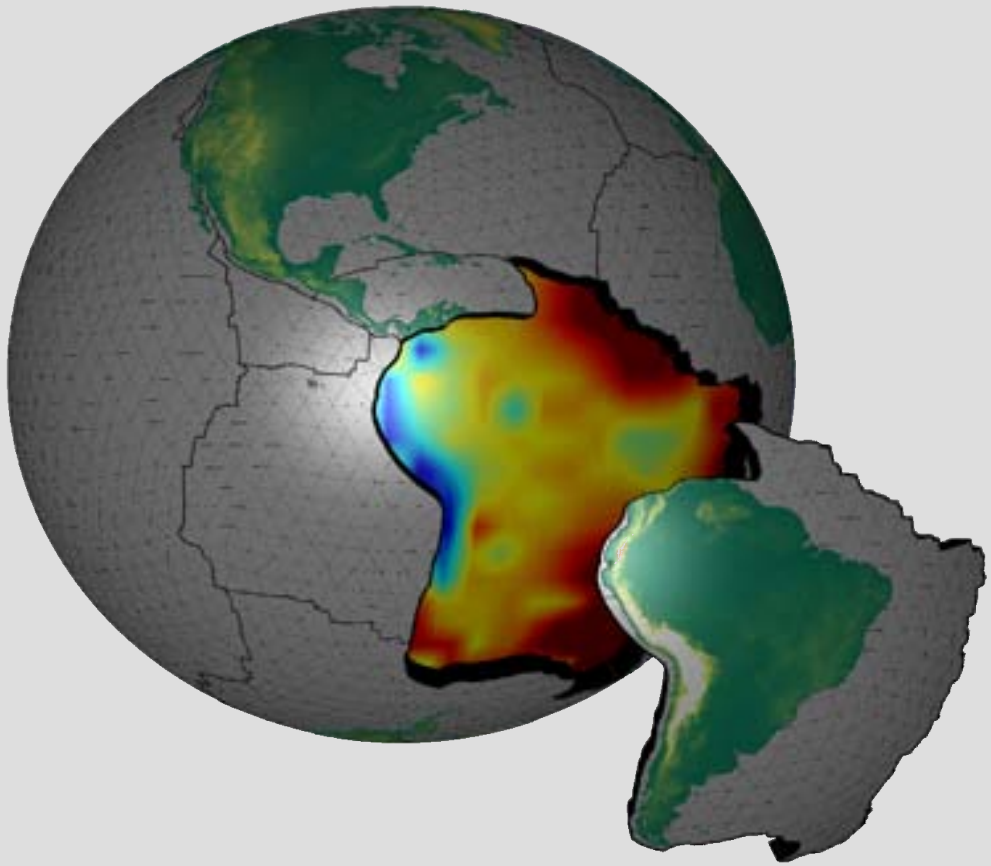

e.g., **Iaffaldano et al. (2006), Iaffaldano & Bunge (2006,2009), Iaffaldano et al. (2011), Austermann & Iaffaldano (2013**

Global **Neotectonic Models** coupled to **Mantle Circulation Models** that include buoyancies from a subduction history

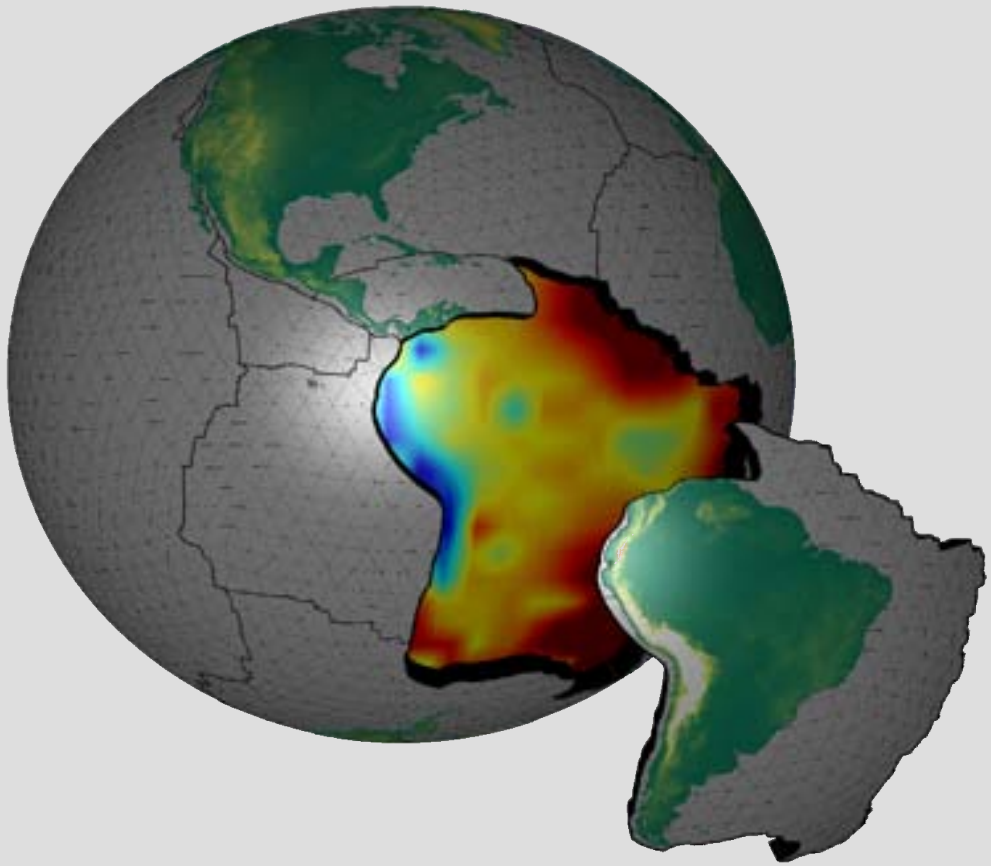

Such models may be used to test parameters explicitly against **Geodetic & Paleomagnetic** observations.

e.g., **Iaffaldano et al. (2006), Iaffaldano & Bunge (2006,2009), Iaffaldano et al. (2011), Austermann & Iaffaldano (2013**

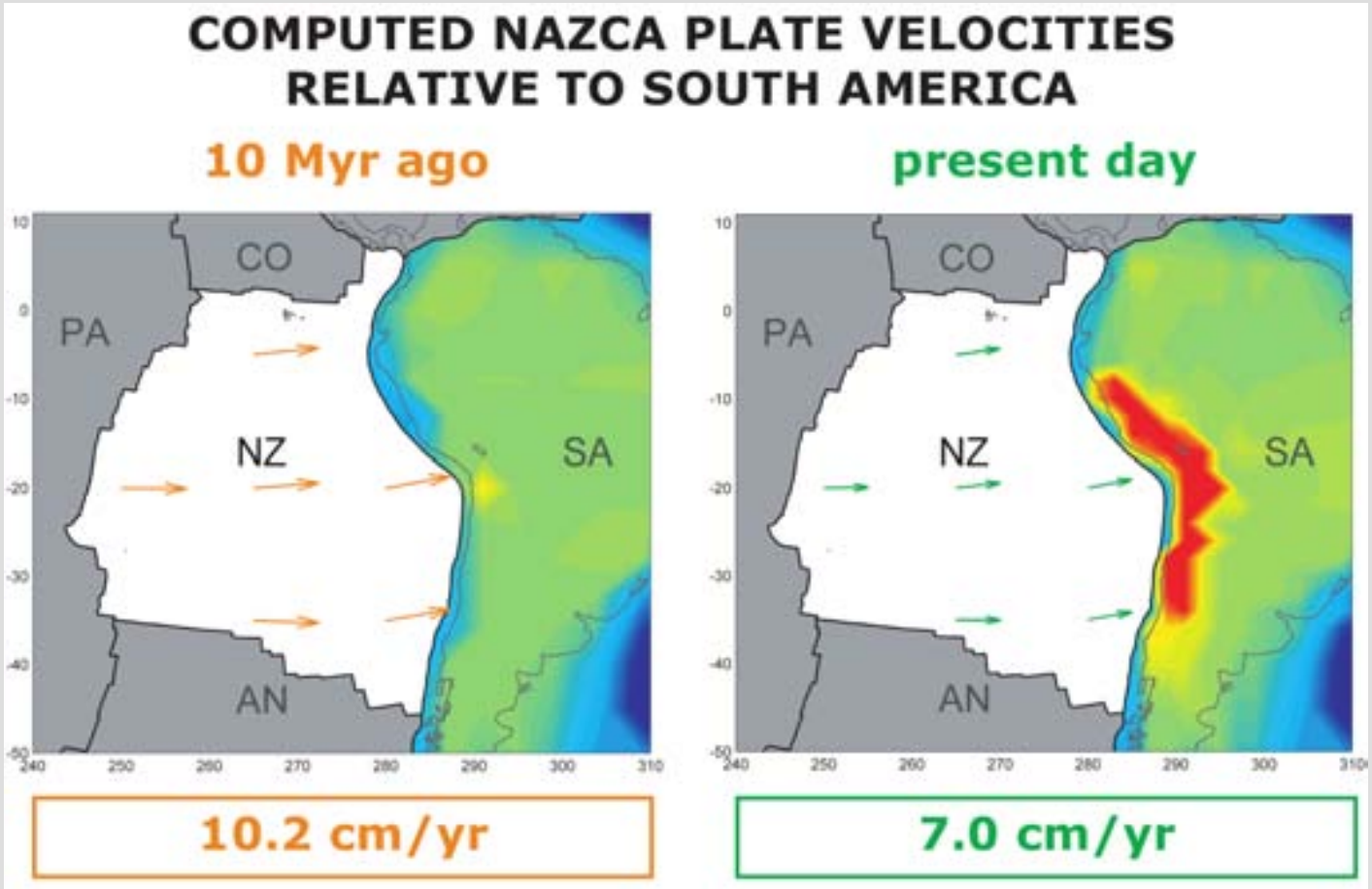

e.g., **Iaffaldano et al. (2006), Iaffaldano & Bunge (2006,2009)**

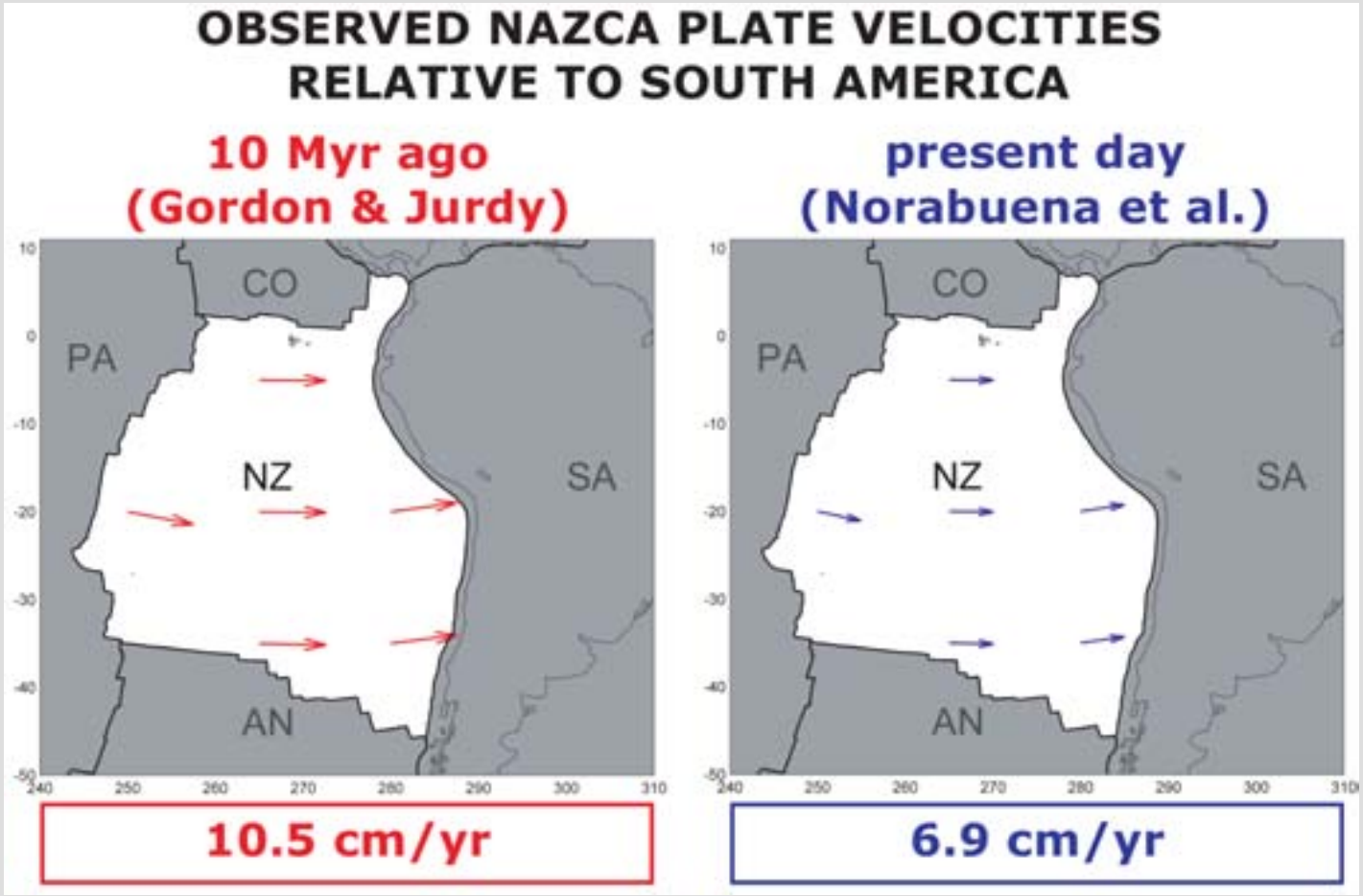
OBSERVED NAZCA PLATE VELOCITIES
RELATIVE TO SOUTH AMERICA
10 Myr ago
(Gordon & Jurdy)
present day
(Norabuena et al.)
CO
PA
NZ
SA
AN
10.5 cm/yr
6.9 cm/yr

Similar effects of topography have been observed and modeled for the recent slow-down of the *Arabian* and *Indian* plate, associated with the rise of the Zagros and Himalaya, respectively.

Topography introduces an **additional time scale** and links known plate motion changes to **forces that can be quantified**.

e.g., **Iaffaldano et al. (2006), Iaffaldano & Bunge (2006,2009), Iaffaldano et al. (2011), Austermann & Iaffaldano (2013**

- **Paleogene**
  South Atlantic Spreading Variations

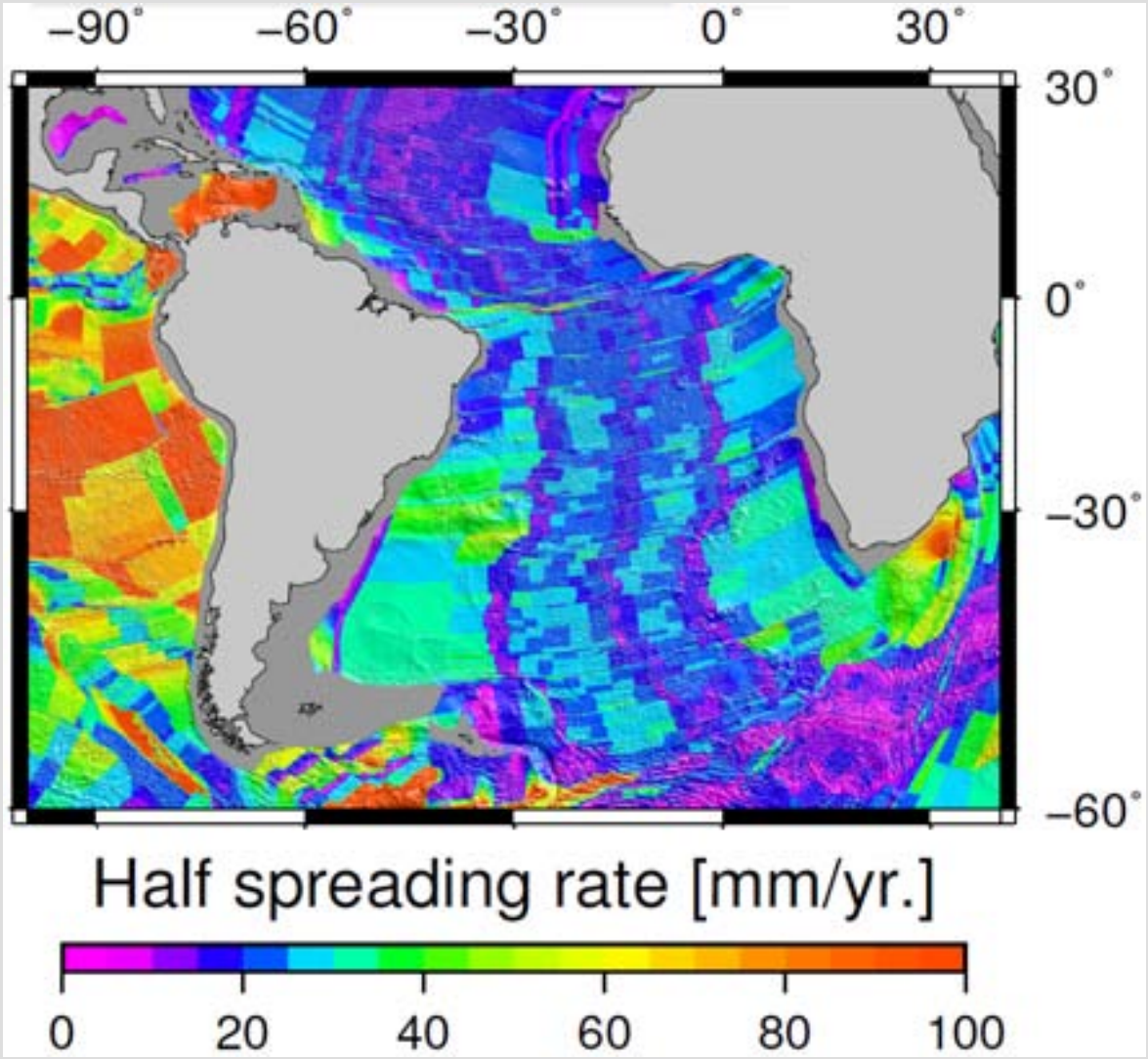

- **Paleogene** South Atlantic Spreading Variations

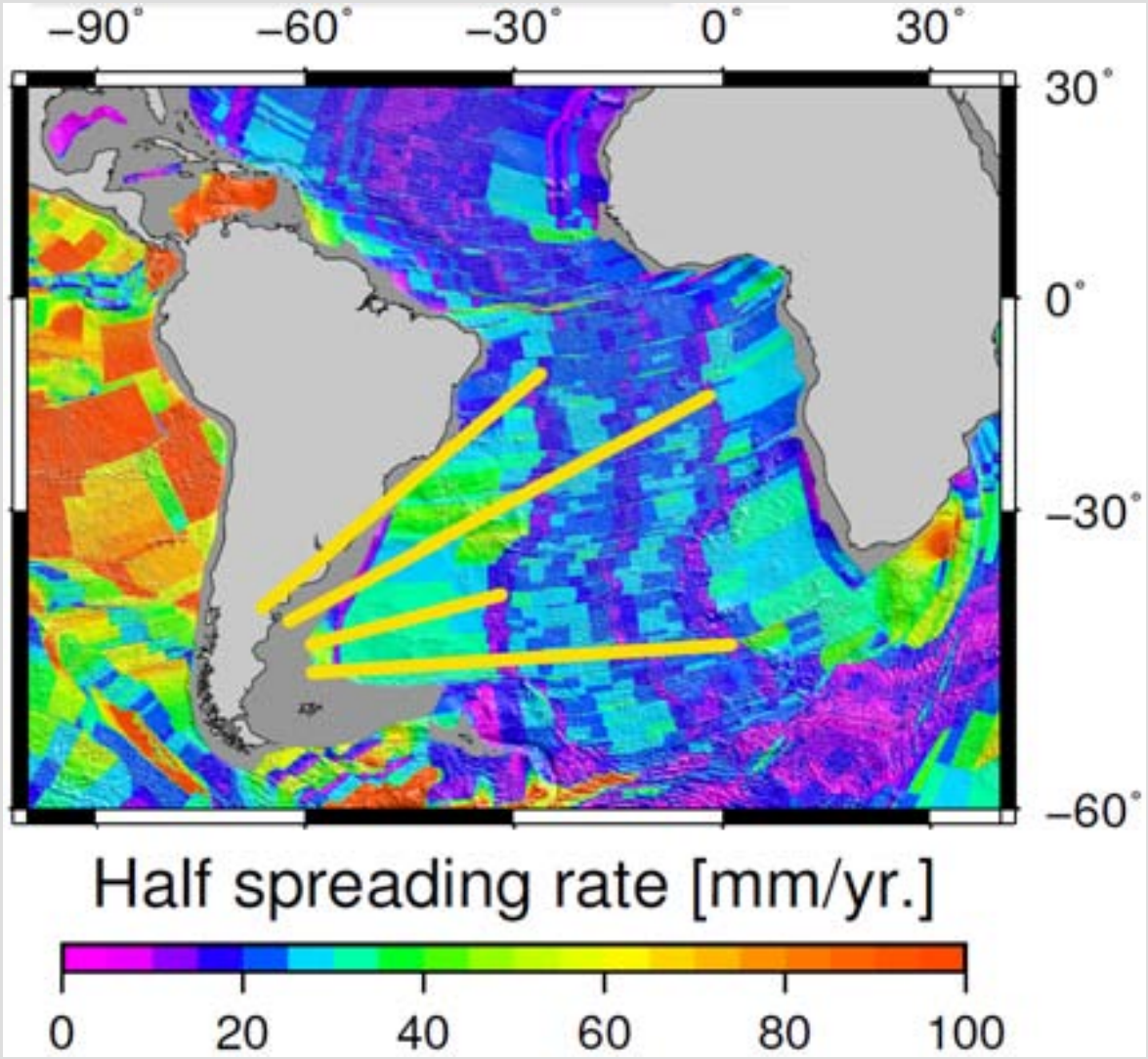

Compare six plate motion models of the South Atlantic

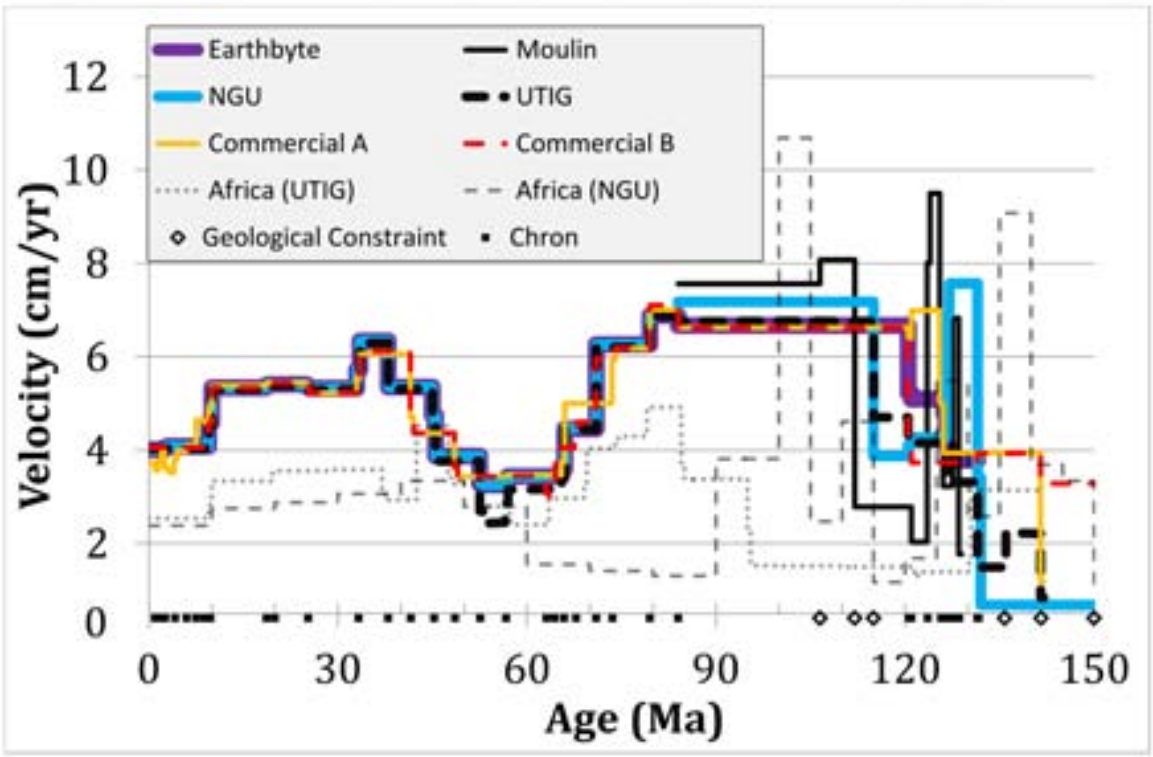

Colli et al. (2014)

Compare six plate motion models of the South Atlantic

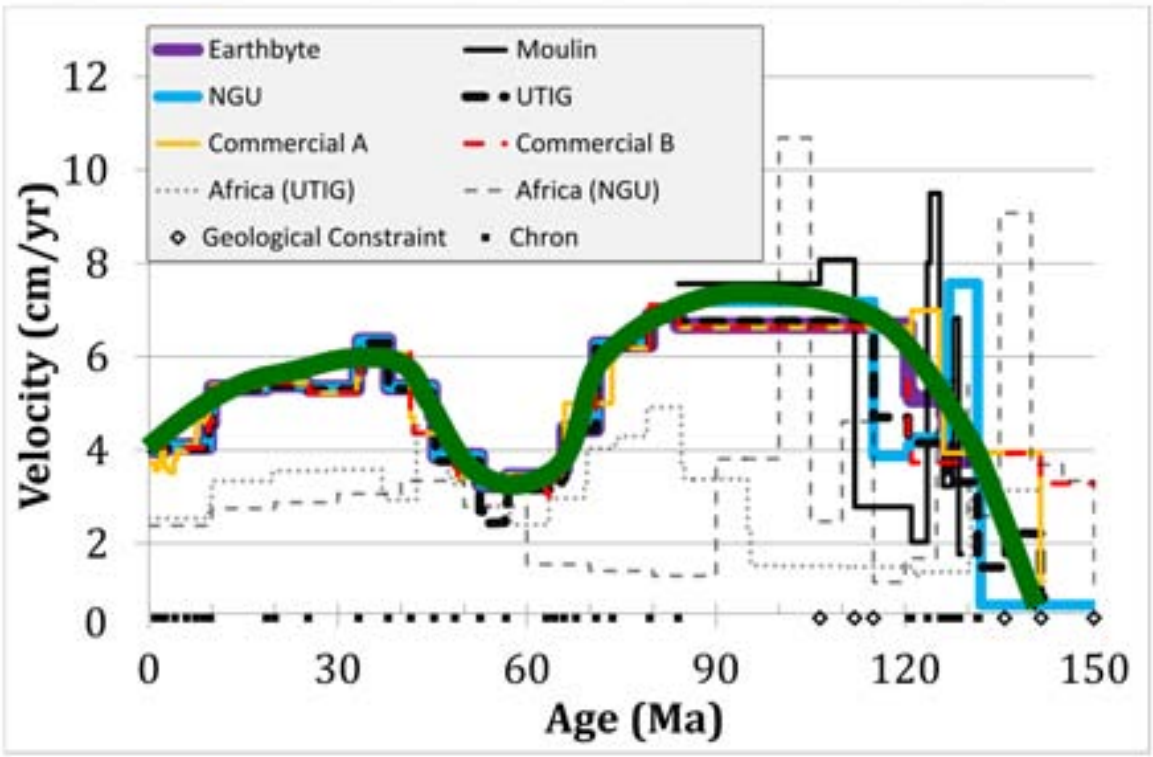

Colli et al. (2014)

Two phases of high velocity: up to 70 Myrs (Late Cretaceous) and between 45 and 10 Myrs (Oligocene – Miocene)

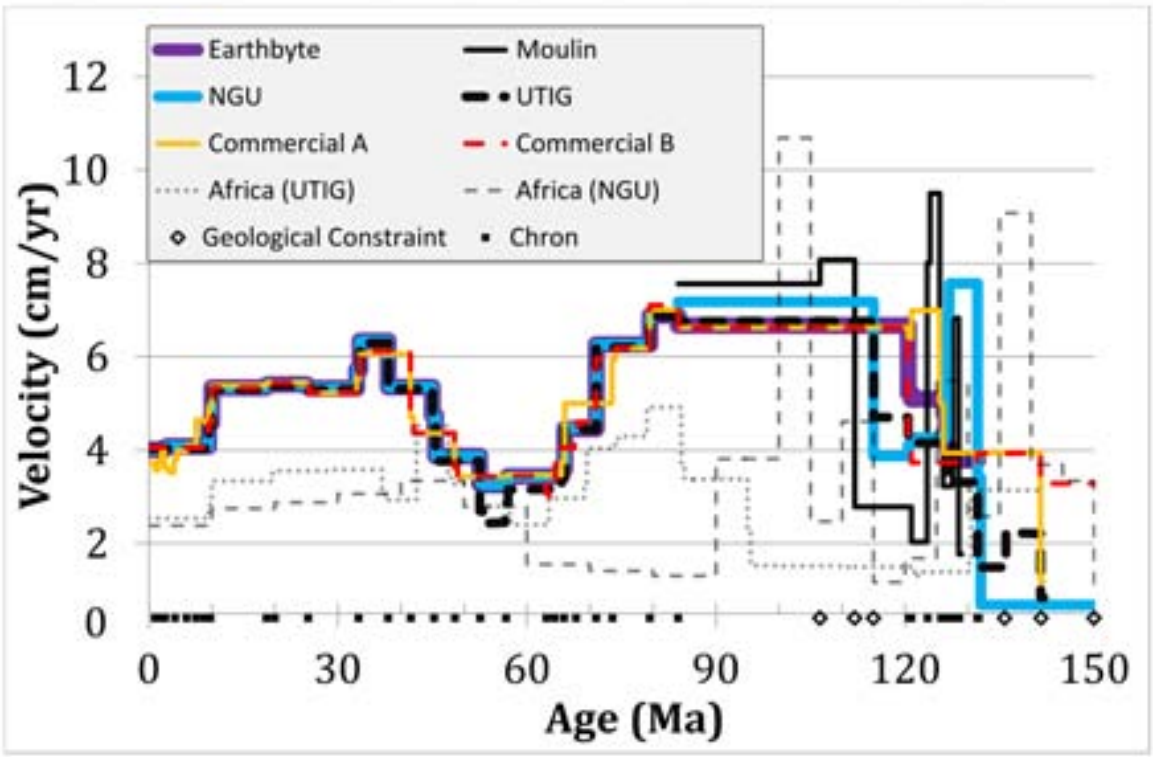

Geologic estimates of Paleo-Andean elevation

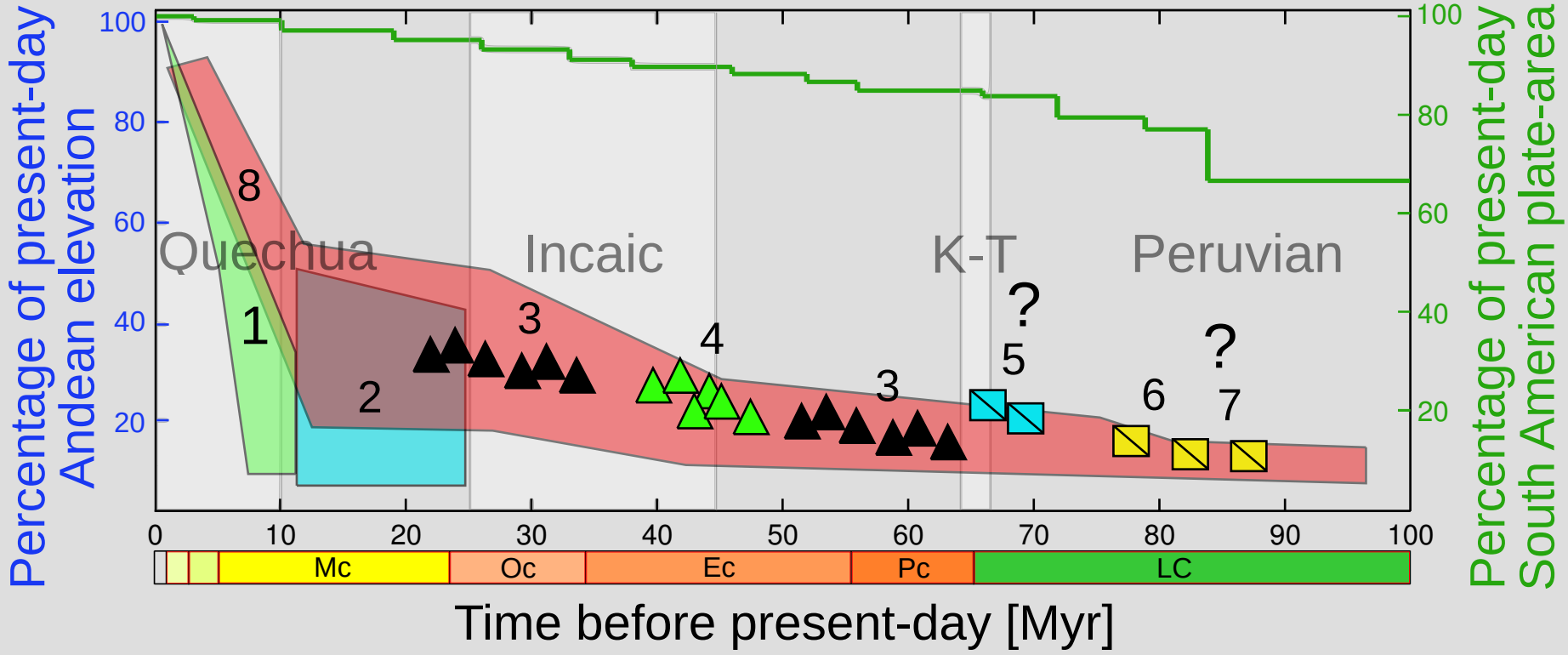

Colli et al. (2014)

upper mantle low viscosity zone (a recurrent theme in Geodynamics)

- linear stability
- planform studies
- stress amplification
- pressure driven flow

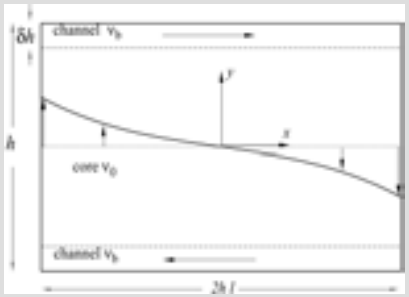

Busse et al. (2006)

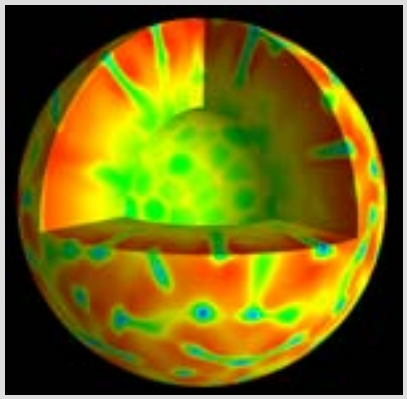

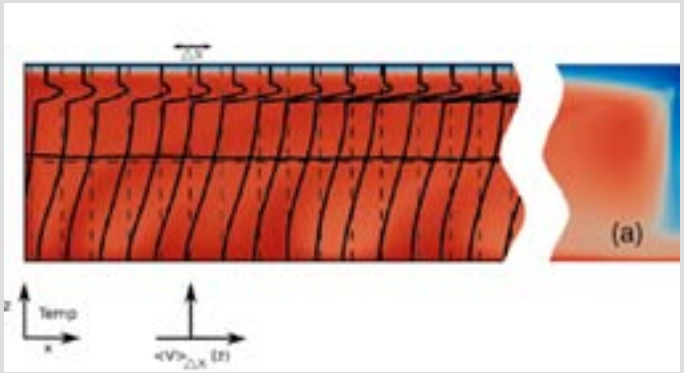

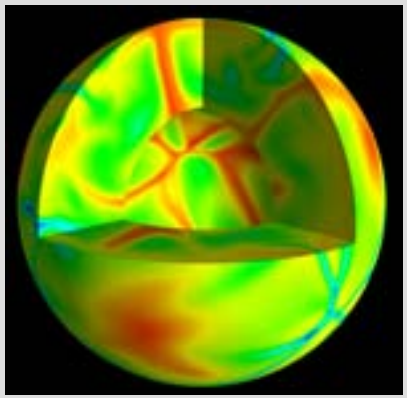

e.g., **Hoeink & Lenardic (2008,2010),**

Hoeink et al. (2011)

Poiseuille/Couette flow types

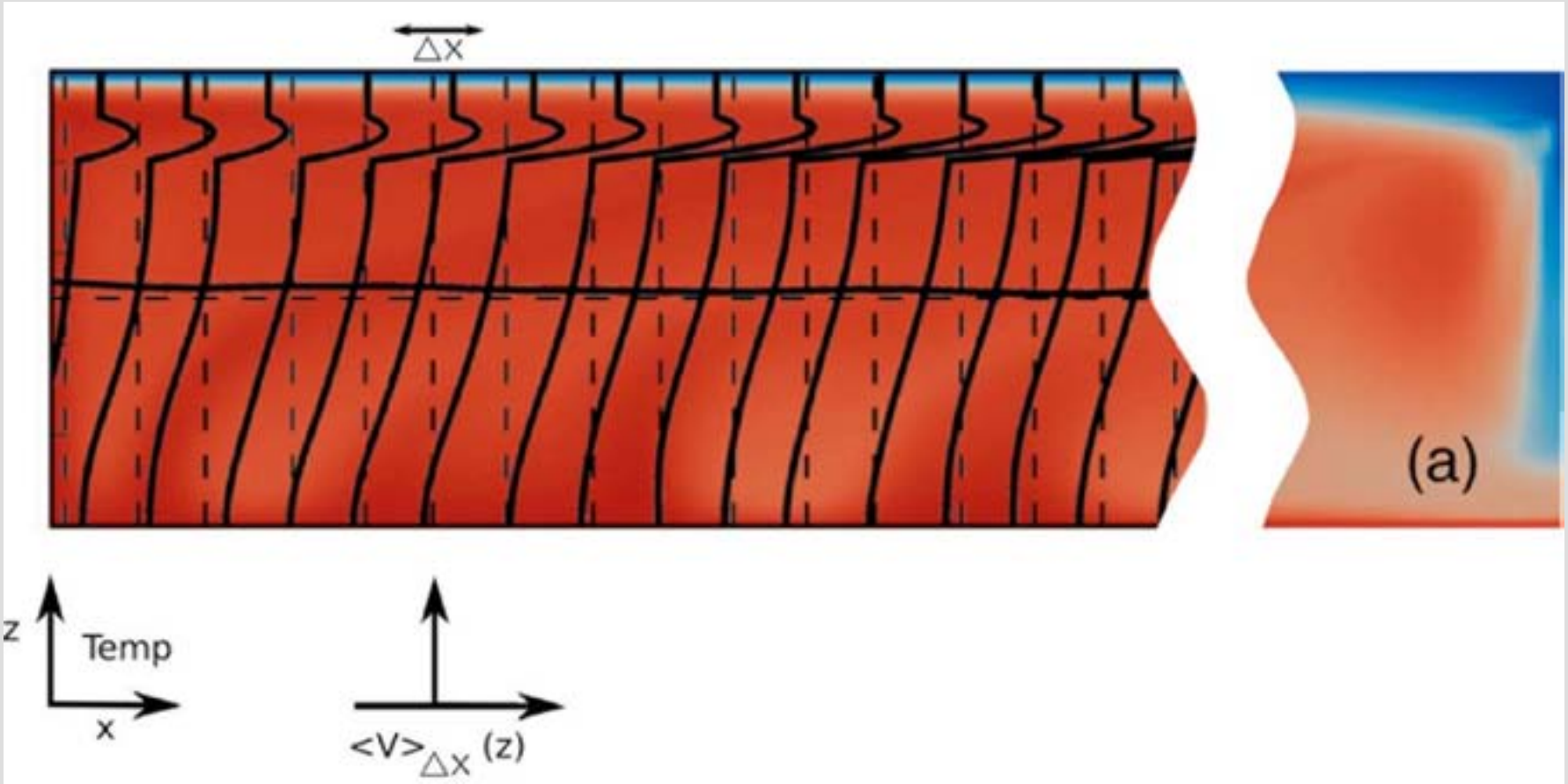

Hoeink et al. (2011)

Poiseuille/Couette flow types

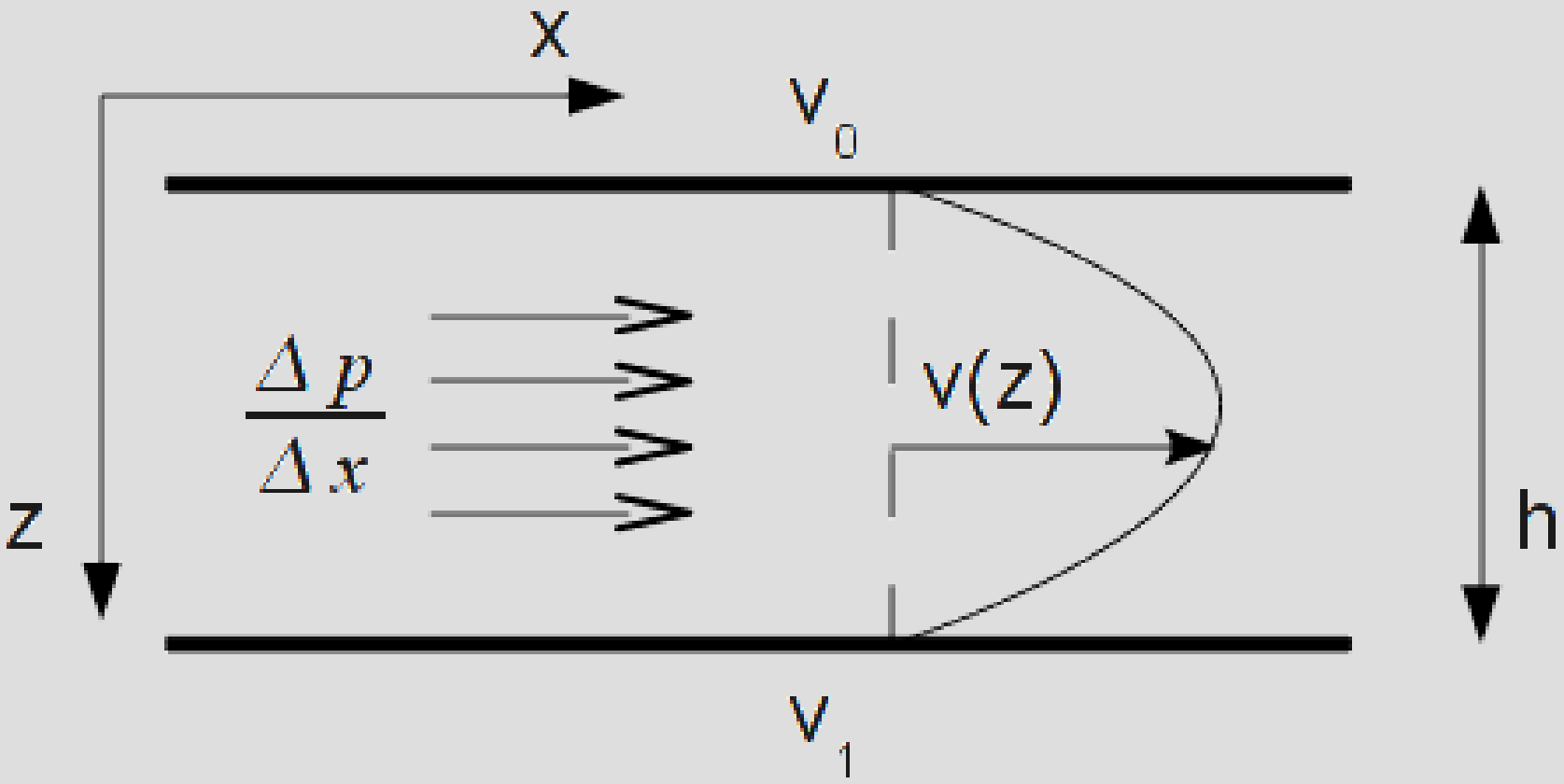

trade-off in layer thickness and viscosity reduction

- models favoring a coarse subdivision of the mantle into two layers separated at 670 km depth naturally obtain *modest* viscosity contrasts, while providing an equally good fit to the data as models with a *thin* layer and *strong* viscosity reduction

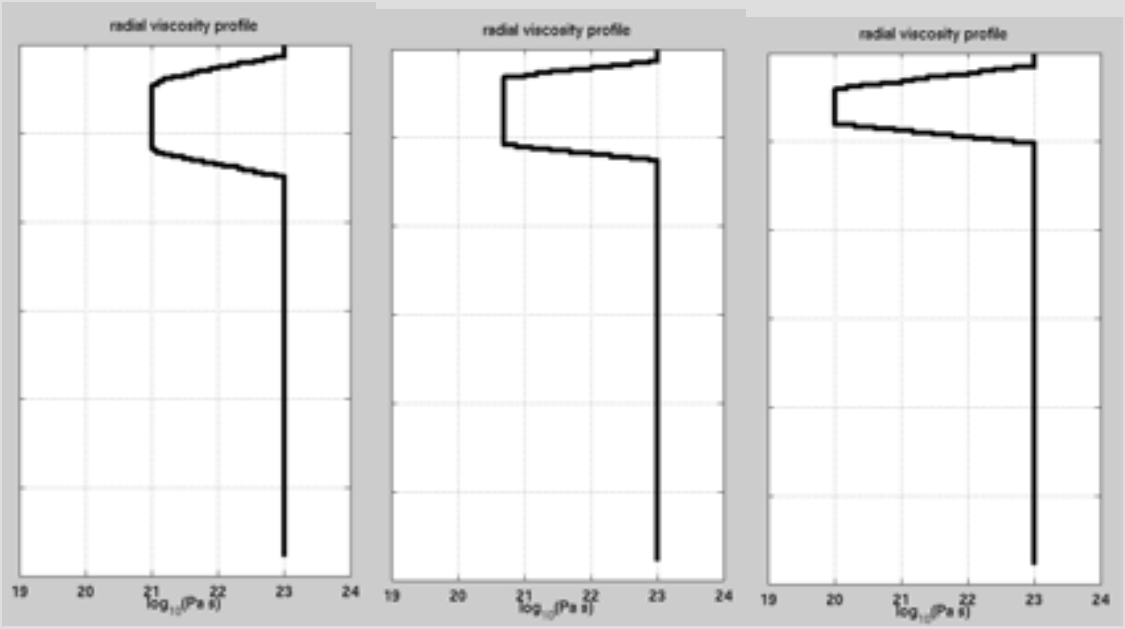

equivalent radial mantle viscosity profiles

trade-off in layer thickness and viscosity reduction

decay time

$$\tau \propto \frac{\mu}{h^3}$$

there is an ensemble of LVZ earth models, having similar values for $\frac{\mu}{h^3}$

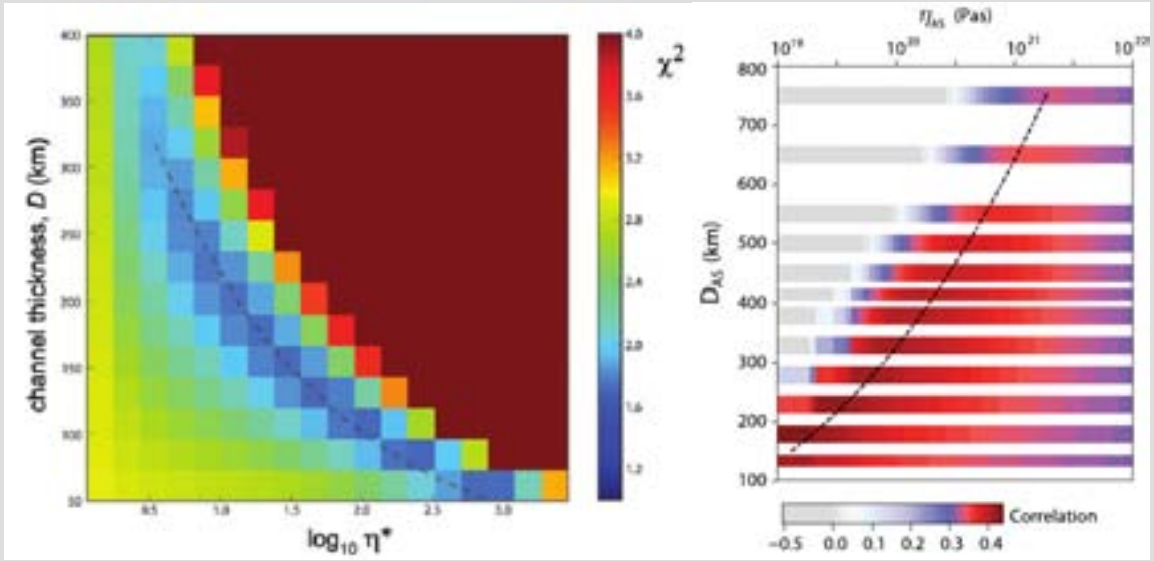

e.g., Paulson & Richards (2009) figure on the left, Schaber et al. (2009) figure on the right

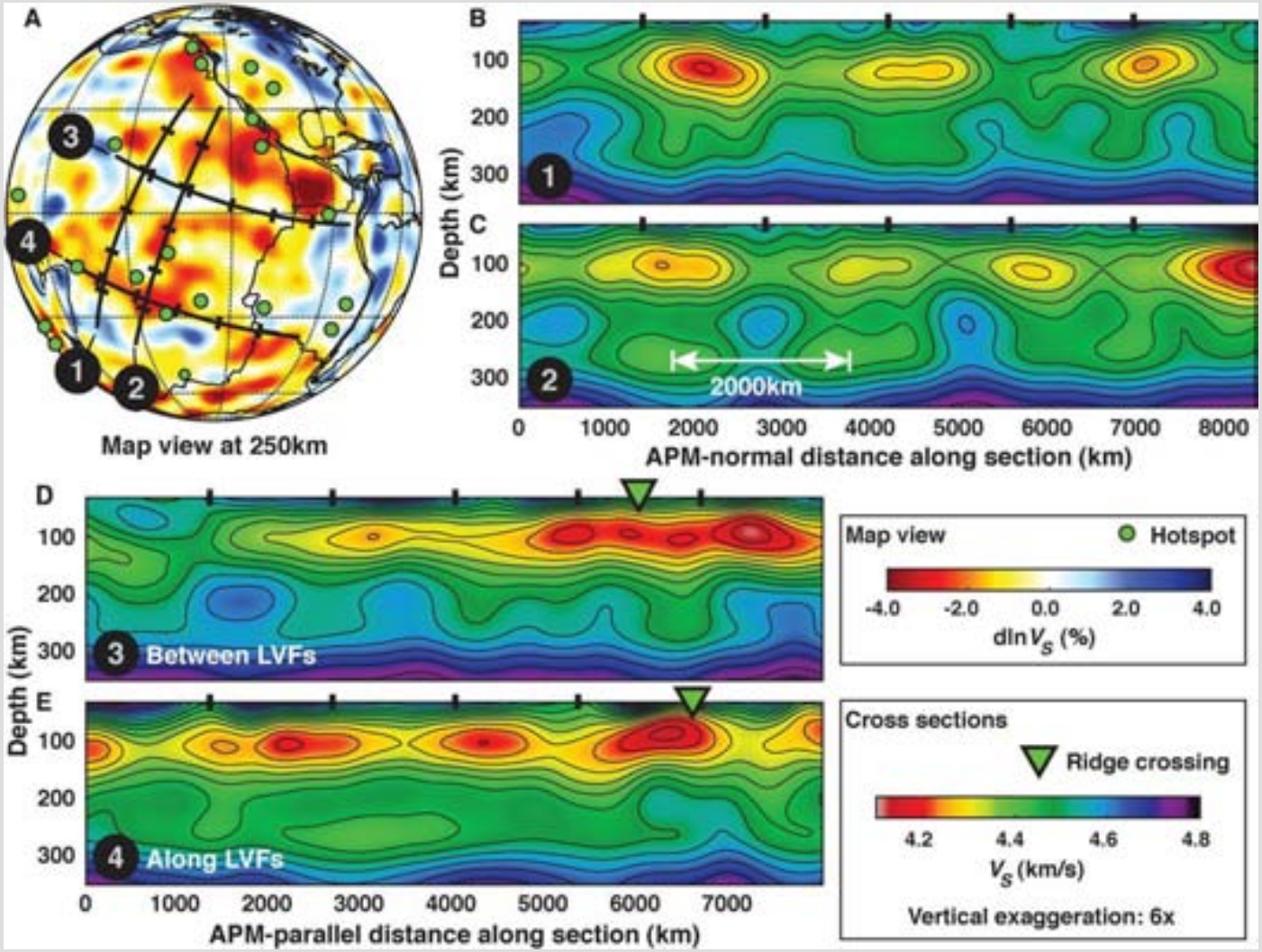

French, Lekić & Romanowicz (2013)

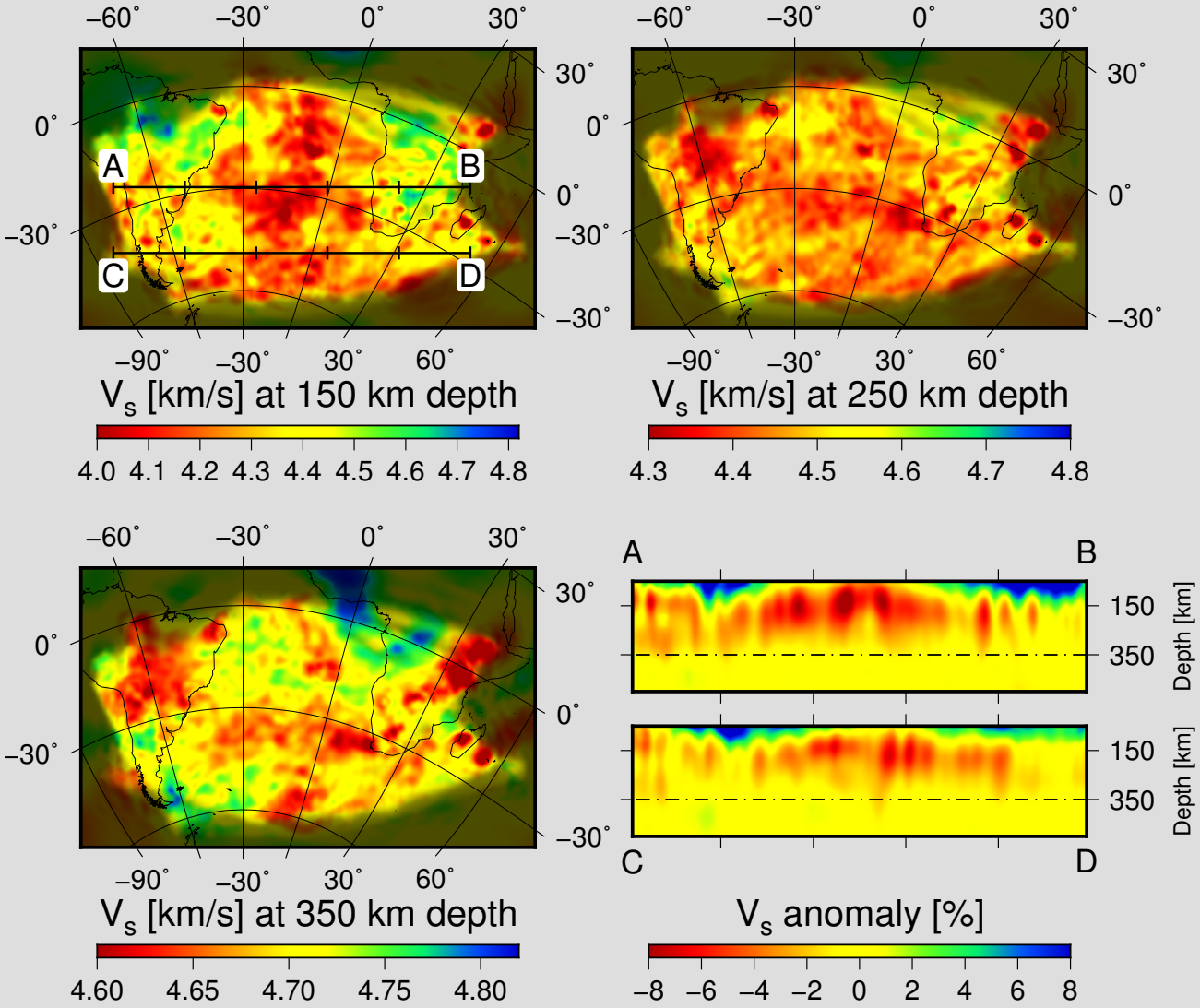

from **Colli et al. (2014)**, also Rickers et al. (2013) in North Atlantic, Fichtner et al. (2009) in Australasian region

Present-day mantle flow inferred through force balance

LVZ velocity values required to balance the current Andean topography by basal shear for a variety of depths of the LVZ. We exclude small (100 km or less) as well as big (400 km or more) depth values for the LVZ.

Viscosity	Asthenosphere channel thickness				
	100 km	200 km	300 km	400 km	500 km
1×10^{18} Pa s					
5×10^{18} Pa s		32.2			
1×10^{19} Pa s		16.9	24.1		
5×10^{19} Pa s			6.1		
1×10^{20} Pa s					

Colli et al. (2014)

Present-day mantle flow inferred through Poiseuille

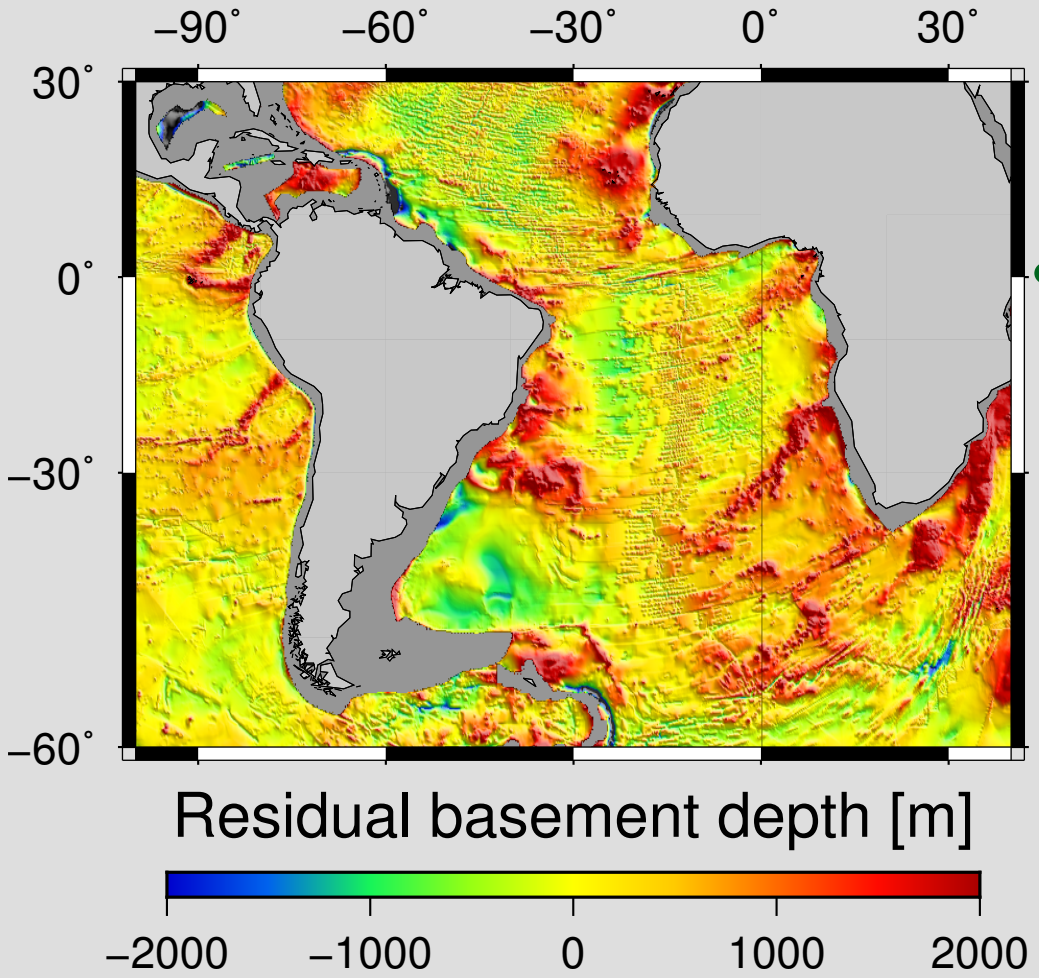

- pressure gradient across the basin:
  600 bar ($\approx$ 2 km of rocks)

Present-day mantle flow inferred through Poiseuille

$$v_x(y) = \frac{1}{\mu}\frac{\Delta p}{\Delta x} y(h-y)$$

- pressure gradient across the basin:
  600 bar ($\approx$ 2 km of rocks)
- Poiseuille flow
- velocity: **6–30 cm/yr**

The two independent estimates of LVZ velocity -based on a *Force Balance* or a *Poiseuille* argument - are in remarkable agreement.

Colli et al. (2014)

Present-day mantle flow inferred through Poiseuille

$$v_x(y) = \frac{1}{\mu}\frac{\Delta p}{\Delta x} y(h-y)$$

- pressure gradient across the basin:
  600 bar ($\approx$ 2 km of rocks)
- Poiseuille flow
- velocity: **6–30 cm/yr**

The two independent estimates of LVZ velocity -based on a *Force Balance* or a *Poiseuille* argument - are in remarkable agreement.

Colli et al. (2014)

Africas Elevation History

- Numereous studies have assigned **Mesozoic** or **Cenozoic** ages to the timing of Africa's togographic high stand.

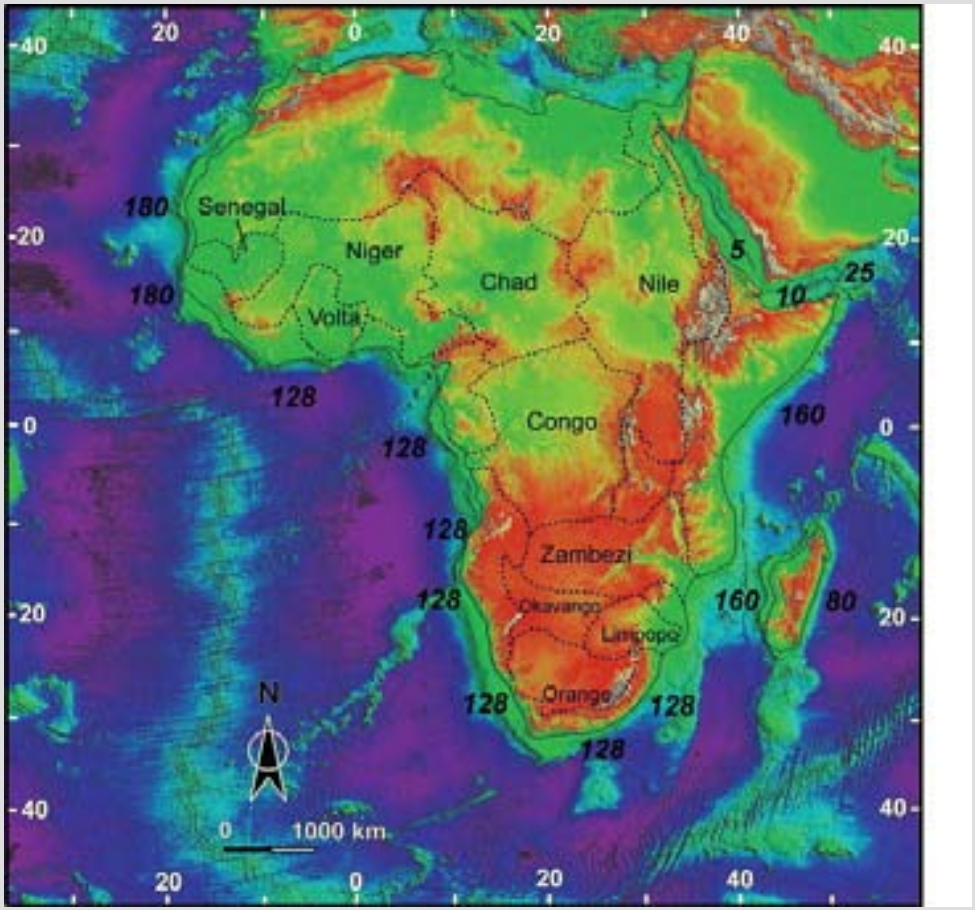

Burke & Gunnell. (2008)

Africas Elevation History

French TopoAfrica program:
Late Cretaceous and Oligocene ⇔ Miocene uplift periods

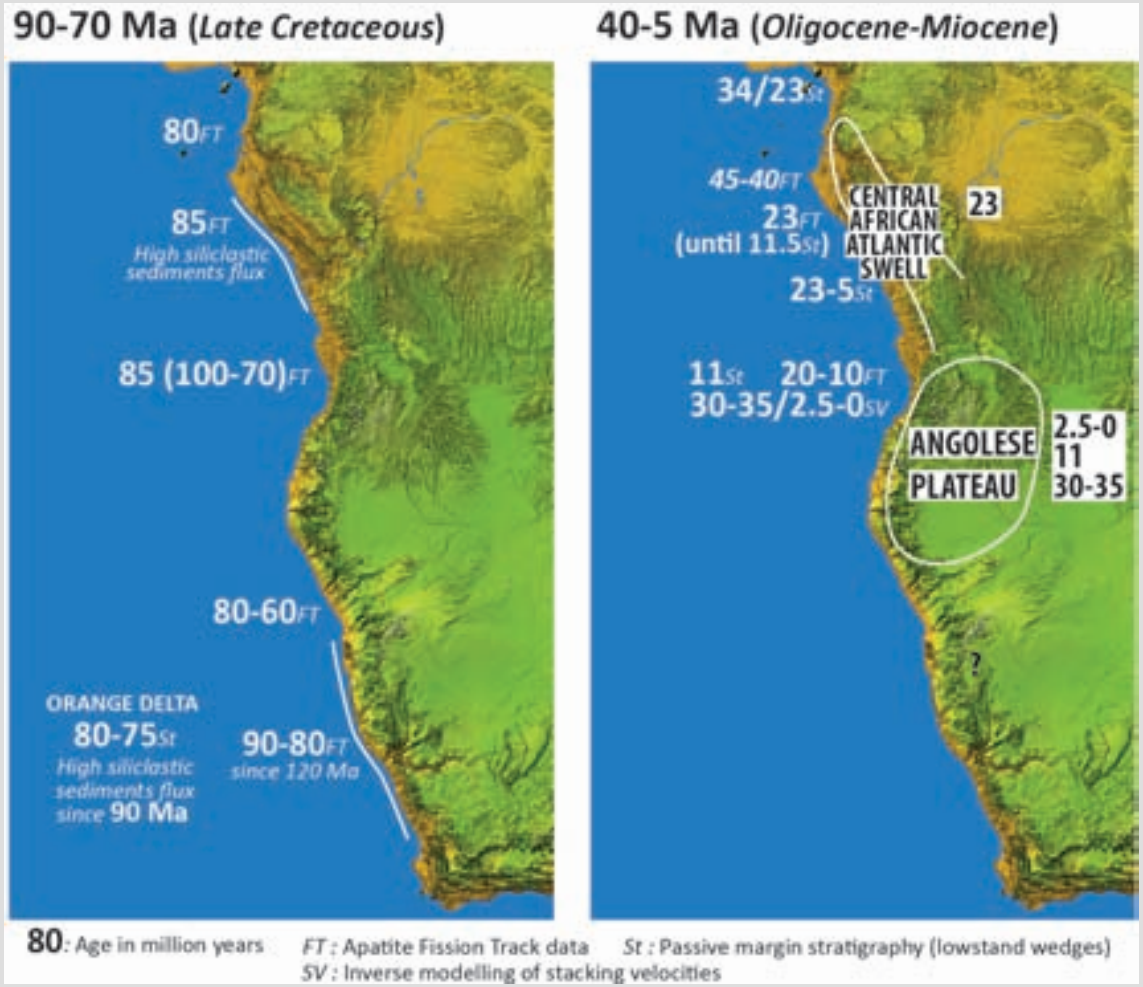

Africas Elevation History

"Kimberlite eruption ages constrains a Mesozoic unroofing pulse, most intense between 100 to 90 Ma, while the apatite (AHe) results also detect as much as 1.5 km of Cenozoic unroofing."

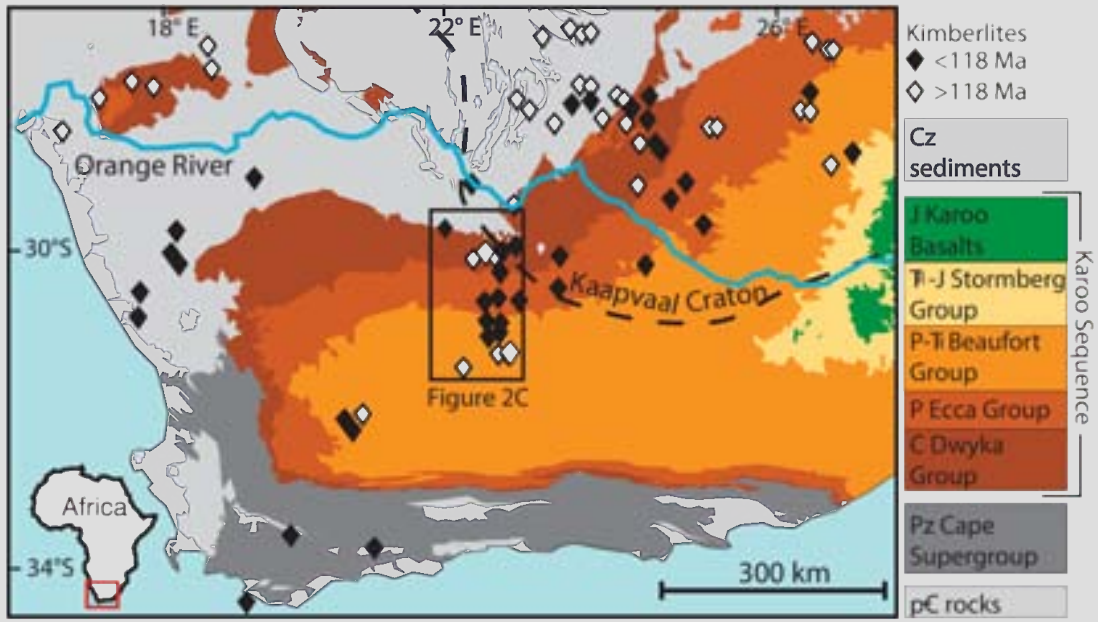

Stanley et al. (2013)

CONCLUSIONS

- Rapid Plate Motion Changes hold key information on plate boundary forces and mantle flow.
- Some plate boundary forces are related to topography.
- Some plate motion changes suggest channelised flow in a thin LVZ layer.
- Poiseuille flows in the asthenosphere link horizontal and vertical motion, i.e. periods of fast spreading and widespread (epeiorogenic) uplift, implying that paleo mantle flow could be inferred from multiple data sets.

Colli et al., Tectonics, Vol 33, 2014

Iaffaldano & Bunge, accepted Annual Reviews, 2015